1 Improved methods and optimized design for CRISPR Cas9 and

2 Cas12a homology-directed repair

3 **Mollie S. Schubert[1], Bernice Thommandru[1], Jessica Woodley[1], Rolf Turk[1], Shuqi Yan[1,2], Gavin**

4 **Kurgan[1], Matthew S. McNeill[1] and Garrett R. Rettig[1,*]**

5 [1] Integrated DNA Technologies, Inc., Coralville, IA, 52241, USA

6 [2] Present address: BGI Genomics, BGI-Shenzhen, Shenzhen 518083, China.

7 * Correspondence should be addressed to G.R.R (Email: grettig@idtdna.com)

8

9 **ABSTRACT**

10 CRISPR-Cas proteins are used to introduce double-stranded breaks (DSBs) at targeted genomic loci.

11 DSBs are repaired by endogenous cellular pathways such as non-homologous end joining (NHEJ)

12 and homology-directed repair (HDR). Providing a DNA template during repair allows for precise

13 introduction of a desired mutation via the HDR pathway. However, rates of repair by HDR are often

14 slow compared to the more rapid but less accurate NHEJ-mediated repair. Here, we describe

15 comprehensive design considerations and optimized methods for highly efficient HDR using single-

16 stranded oligodeoxynucleotide (ssODN) donor templates for several CRISPR-Cas systems including

17 *S.p.* Cas9, *S.p.* Cas9 D10A nickase, and *A.s.* Cas12a delivered as ribonucleoprotein complexes with

18 synthetic guide RNAs. Features relating to guide RNA selection, donor strand preference, and

19 incorporation of blocking mutations in the donor template to prevent re-cleavage were investigated

20 and were implemented in a novel online tool for HDR donor template design. Additionally, we employ

21 chemically modified HDR donor templates in combination with a small molecule to boost HDR

22 efficiency up to 10-fold. These findings allow for high frequencies of precise repair utilizing HDR in

23 multiple mammalian cell lines. Tool availability: www.idtdna.com/HDR

24

25 **INTRODUCTION**

26 CRISPR-Cas systems have revolutionized genomics by enabling efficient and precise genome editing

27 in a wide variety of biological systems, including eukaryotic cells.[1-5] These systems require an RNA-

28 guided DNA endonuclease and a target-specific guide RNA (gRNA) to generate a double-stranded

29 break (DSB) at a desired genomic location, which must be flanked by a short protospacer adjacent

1

30   motif (PAM). *Streptococcus pyogenes* Cas9 (*S.p.* Cas9) is one of the most commonly used CRISPR

31   enzymes for genome editing. The native gRNA for Cas9 is hybridized from two RNA molecules: a

32   CRISPR RNA (crRNA) and a universal, trans-activating crRNA (tracrRNA).[6] The two strands of the

33   gRNA can also be combined as a single unimolecular structure to form a single-guide RNA (sgRNA).[7]

34   Association of Cas9 protein with a gRNA forms a ribonucleoprotein (RNP) complex, which surveys a

35   dsDNA substrate and generates a DSB when its complementary target sequence with a PAM is

36   recognized by an active Cas9 RNP complex.[8-10]

37   Recent reports have demonstrated that RNP delivery of nucleases has benefits over plasmid delivery

38   as it enables a faster onset of action, reduces off-target cleavage, and eliminates the risk of random

39   plasmid integration into the host genome.[9,11,12] At the same time, RNP delivery allows for the use of

40   chemically modified gRNA with improved stability and reduced toxicity.[13] In addition, generating RNP

41   complexes *in vitro* prior to delivery allows accurate control of the ratio of protein and gRNA to

42   maximize RNP complexation efficiency. This also enables the formation of each gRNA:protein

43   complex independently which mitigates the competition for Cas9 protein by other intracellular RNA

44   molecules or by different gRNAs during multiplexing experiments.[14]

45   *S.p.* Cas9 contains two endonuclease domains (HNH and RuvC) that function together to generate a

46   blunt DSB by each domain cleaving opposite DNA strands. Inactivating one of the two endonuclease

47   domains results in Cas9 variants called "nickases": the RuvC-inactive variant (Cas9 D10A) nicks the

48   target (gRNA complementary) strand, while the HNH-inactive variant (Cas9 H840A) nicks the non-

49   target (gRNA non-complementary) strand.[7] Cas9 nickases can be used with an individual guide to

50   induce single DNA nicks and induce a repair pathway termed alternative-HDR.[15,16] However, it is

51   more common and often more efficient to perform genome editing at DSBs generated by using a

52   nickase with a pair of gRNAs targeting opposite DNA strands in a "paired nicking strategy".[17] It has

53   been demonstrated that nickases allow for the reduction of off-target editing by ~50-1500 fold in

54   comparison to Cas9 WT.[17-19] At the same time, the paired nicking strategy can facilitate highly robust

55   editing in many model systems, including mammalian tissue culture, mouse zygotes, plants, yeast,

56   and bacteria.[1,17-26]

57   Cas12a enzymes are also RNA-guided double-stranded DNA nucleases that provide an alternative to

58   the commonly used *S.p.* Cas9 nuclease with similar editing outcomes. Unlike *S.p.* Cas9, which

59   recognizes an NGG PAM sequence, *A.s.* Cas12a recognizes a TTTV (V = A/G/C) PAM site which

60   allows for a broadened range of targeting sites in AT-rich regions. Cas12a relies on a single, short

61   (41-44 nt) gRNA and generates staggered DSBs with 5' overhangs.[4] In addition, Cas12a has been

62   shown to be advantageous due to intrinsically high specificity, reducing the potential for off-target

63   cleavage.[27,28] However, Cas12a also has non-specific single-stranded DNase (ssDNase) activity that

64   is activated upon binding to the target DNA strand.[29] This could potentially impact the ability of

65   Cas12a to mediate efficient HDR if the ssODN is degraded before it is able to act as a donor

66   template.

67   To facilitate genome editing, CRISPR-Cas enzymes are used to generate a DSB at a genomic locus

68   which can then be repaired by a variety of endogenous cellular repair pathways including non-

69   homologous end joining (NHEJ) and homology-directed repair (HDR).[30,31] NHEJ is an imperfect

70   process and commonly creates small insertions or deletions (indels), which can be exploited to

71   introduce diverse, but reproducible genetic mutations or gene knockouts.[32] On the other hand, HDR is

72   a process that can lead to precise sequence alterations at specified genomic locations but requires

73   the use of a carefully designed HDR donor template that contains sequences homologous to the

74   specific sequence flanking the cut site, defined as 'homology arms'. However, rates of repair by HDR

75   are often slow compared to the more rapid but less accurate NHEJ-mediated repair.[33] For small

76   mutations or insertions, a ssODN can be used as the HDR donor template.[34-37] These are readily

77   available up to 200 nucleotides (nt) in length as chemically synthesized oligos, allowing for insertions

78   up to 160 nt (maintaining, at minimum, 20-nt homology arms).

79   Two distinct pathways for the incorporation of single-stranded donor templates at a DSB have been

80   proposed – single-strand DNA incorporation (ssDI) and synthesis-dependent strand annealing

81   (SDSA), with SDSA being preferentially utilized as the repair path for ssODN donor templates in the

82   presence of a DSB.[38] Previous studies have examined design considerations for ssODNs when using

83   CRISPR-Cas enzymes. The optimal length of homology arms has been reported to be as little as 30-

84   nt in length on either side of the DSB, and it has been demonstrated that asymmetric donor oligos can

85   improve HDR.[39,40] HDR efficiency is highest when the intended edit is placed near the DSB and is

86   greatly reduced at loci distal to this event.[35,41] In addition, reports have indicated that there may be a

87   preference for utilizing a donor oligo with sequences either complementary or non-complementary to

88   the gRNA.[37,42-44] CRISPR-Cas9 can also re-cut dsDNA after a desired repair outcome if the

3

89   protospacer and PAM sequence remains unaltered, lowering perfect HDR efficiency. This outcome

90   can be prevented by strategically incorporating blocking mutations into the donor template.[35,45]

91   Other approaches to improving HDR are of great interest to the genome editing community. It has

92   been previously reported that incorporating chemical modifications such as phosphorothioate (PS)

93   linkages may improve HDR when using ssODN donors.[39,46] Another route to improving HDR

94   frequency is using chemical compounds that inhibit key DSB repair enzymes that play a role in the

95   competing NHEJ pathway. Several chemical compounds have been reported to increase HDR.[47-49]

96   In this work, we thoroughly investigated design features for both *S.p.* Cas9 and *A.s.* Cas12a

97   nucleases relating to gRNA selection, donor strand preference, the placement and composition of

98   blocking mutations, and the number of blocking mutations that are required for maximum HDR

99   efficiency. We additionally investigated alternate end-blocking oligo modifications to further stabilize

100   the ssODN from exonuclease activity and have developed a novel modification, which is incorporated

101   into Alt-R HDR Donor Oligos, that improves upon previously reported constructs. Here, we

102   demonstrate that the use of end-modified Alt-R HDR Donor Oligos along with Alt-R HDR Enhancers,

103   small molecules that inhibit NHEJ-mediated repair, combine to significantly increase the rate of HDR

104   when delivered with CRISPR RNP complexes in mammalian cell lines. Altogether, this study presents

105   a set of design considerations and reagents which can be applied to CRISPR editing experiments to

106   maximize HDR efficiency and reduce time spent generating desired mutants. Our findings constitute

107   an empirically defined ruleset for *S.p.* Cas9 and *S.p.* Cas9 D10A nickase which have been built into a

108   novel bioinformatic tool for HDR donor template design. Further, we provide design recommendations

109   for *A.s.* Cas12a nuclease, which has not yet been systematically studied in the same manner as

110   Cas9.

111

112   **RESULTS**

113   **Cas9 donor strand preference and gRNA selection**

114   While some studies have suggested that there is a strand preference for the ssODN donor template,

115   where one strand's homology sequence consistently mediates improved HDR frequency over the

116   other strand, results have varied and no universal strand preference has been identified.[37,42-44] To

117   elucidate any universal strand preference of the HDR donor template with WT Cas9 nuclease,

118   particularly when delivered as an ribonucleoprotein (RNP) complex, HDR efficiency was tested at 254

4

119   genomic loci in Jurkat cells and 239 genomic loci in HAP1 cells. Donor ssODNs containing 40-nt

120   homology arms were designed to insert a six base EcoRI restriction digest recognition site

121   ('GAATTC') at the Cas9 cleavage site which canonically lies three bases in the 5' direction of the

122   PAM, as illustrated in Figure 1A. ssODNs were delivered to Jurkat and HAP1 cells along with their

123   respective Cas9 RNP complex by nucleofection, and the editing frequencies were assessed by next

124   generation sequencing (NGS). Perfect HDR, defined as the precise insertion of the EcoRI sequence

125   at the canonical cut site and otherwise maintaining the WT sequence, was quantified and

126   comparisons were made between donor templates consisting of either the targeting strand (T), which

127   is complementary to the CRISPR-Cas9 gRNA, or the non-targeting strand (NT), which contains the

128   'NGG' PAM sequence. In Jurkat cells there was no statistical difference ($p > 0.05$, paired t-test) in total

129   editing when either the T or NT strand was used. However, a significant difference in editing efficiency

130   ($p < 0.0001$, paired t-test) was observed in HAP1 cells where the mean editing was 80.2% when the

131   NT strand was used and 67.8% when the T strand was used, indicating that the T strand may bind to

132   the Cas9 RNP complex and reduce overall editing efficiency within the cellular environment, as

133   suggested by others (Supplemental Figure 1A).[36] As demonstrated in the top two panels of Figure 1B,

134   the strand that leads to higher frequencies of HDR varies depending on the genomic locus and cell

135   type being used. HAP1 cells had HDR frequencies ranging from 0 to 51.1% with a significantly higher

136   mean HDR frequency when the NT strand was used (20.6%) than the T strand (15.2%) ($p < 0.0001$,

137   paired t-test), likely due to the reduced total editing when the T strand was used. In contrast, we

138   observed significantly higher mean HDR frequencies in Jurkat cells when the T strand was used than

139   when the NT strand was used (11.3% vs 7.5%, respectively) ($p < 0.0001$, paired t-test). Overall, HDR

140   efficiency in HAP1 cells was higher than in Jurkat cells, with mean HDR frequencies of 17.9% and

141   9.4%, respectively. In addition, the bottom two panels of Figure 1B show that although efficient total

142   editing is required for HDR to occur, high editing does not always lead to high HDR insertion at each

143   site tested. For example, even though 53% of the sites tested in HAP1 cells and 74% of the sites

144   tested in Jurkat cells had >90% total editing, there is a broad range of HDR frequencies which varied

145   from 0 to 60% among these highly edited loci for both the NT and T strands. This emphasizes the

146   value of testing multiple guides to determine which have the highest potential HDR frequency prior to

147   any experiment where precise genome modification by HDR is desired.

5

148   To investigate the balance between guide cleavage efficiency and distance of the desired HDR

149   mutation to the cut site, we selected 13 guides flanking the stop codon of GAPDH to determine which

150   led to the highest HDR insertion frequency of an EcoRI site just upstream of the 'TAA' stop codon.

151   These guides had cut sites that ranged from 2 to 22 bases from the desired insertion position (Figure

152   1C). The available guides in the nearby region included PAMs on both strands of the genomic DNA,

153   and ssODNs for both the targeting and non-targeting strand were designed and tested in K562 and

154   HEK293 cells for their ability to mediate HDR. As shown in Figure 1D in K562 cells, guides with low

155   editing efficiency yielded low HDR insertion, even if the cut site was close to the desired insertion

156   location. For example, the guide that cuts two bases from the desired insertion (-2) had 32.1% total

157   editing of which 12.6% was HDR insertion (NT strand). Similarly, the guide that cuts five bases from

158   the desired insertion (-5) had 10.7% total editing and only 1.1% HDR insertion. In contrast, the guides

159   that cut 14 and 6 bases from the desired insertion (-14, +6) had 96.0% total editing of which 40.7%

160   was HDR insertion (NT strand) and 87.8% total editing of which 39.7% was HDR insertion (NT

161   strand), respectively. As determined by NGS, these guides had the highest total editing and HDR

162   insertion rates, even though they were further from the desired insertion. This case study indicates

163   that guide efficiency is a critical factor for efficient HDR, and guide selection that is as close as

164   possible to the desired HDR mutation is a secondary consideration. This was also observed in

165   HEK293 cells, where a guide that cuts 6 bases from the insertion (+6: 97% total editing, 34% HDR)

166   led to higher HDR than guides 2 or 5 bases from the insertion (-5: 34.7% total editing, 12.7% HDR; -2:

167   62.2% total editing, 22.4% HDR). This effect was less prominent using guides further from the desired

168   insertion site (e.g. -14) in HEK293 cells, which may be due to differences in the available repair

169   machinery and capacity for HDR in each cell type (Supplemental Figure 1B).

170   We performed a similar experiment at a second genomic locus (TNPO3) in HEK293 cells to further

171   examine factors influencing HDR (Supplemental Figure 1C). The total editing was high for nearly all

172   guides tested in this experiment. However, for a guide with a cut site 9 bases from the desired

173   insertion location (-9) the total editing was 92.6%, and this site yielded reduced HDR efficiency of

174   7.0% compared to the guide that cut one base further from the desired insertion (-10) with an

175   increased 98.5% total editing that also gave an increased HDR insertion frequency of 24.2% with the

176   NT strand, further supporting that guide activity can be more impactful on HDR efficiency than optimal

177   positioning with respect to the cut site.

6

178

Cas9 D10A mediates efficient HDR distant from nick sites

In comparison to WT Cas9, which needs only one gRNA to cut both strands of the target DNA, Cas9 D10A and H840A nickases can be used with paired guides to generate a DSB to mediate genome editing. To facilitate a DSB, the guides must target opposite strands of the genomic DNA and can be oriented with their PAM sites facing toward each other (PAM-in), or apart from each other (PAM-out) (Supplemental Figure S2A). Guides that target the same DNA strand where one PAM site would face in and the second would face out would not be generate a DSB (unless the two nickase variants, D10A and H840A, were used in combination which significantly complicates the experiment). Consistent with other reports utilizing Cas9 nickase variants expressed from a plasmid,[17,21] we found a higher rate of indel formation when D10A and H840A nickases were designed in a PAM-out orientation, and the nickases must be placed with optimal spacing between the nick sites to mediate efficient editing (Supplemental Figure S2B). Here, we designed a set of paired guides against the human *HPRT1* gene with either PAM-out or PAM-in orientation and target nick sites separated by 18–130 bp. We specifically selected gRNAs that have >40% editing efficiency (data not shown) when delivered with WT Cas9 as RNP into HEK-293 cells, to rule out the possibility that poor editing by the nickase RNP pair is caused by poor cleavage efficiency mediated by individual gRNA. The optimal distance (>40% editing as determined by T7EI) between the two nicks was 40-68 nt for Cas9 D10A, and 51-68 nt for Cas9 H840A. For the PAM-out pair with nicks 68-nt apart, the editing was 86.3% with Cas9 D10A and 77.6% with Cas9 H840A. This was reduced to 29.8% and 2.7%, respectively, when the nicks were 85-nt apart. Similarly, for Cas9 H840A, the editing was 74.7% when the nicks were spaced 51-nt apart, and this was reduced to 34.6% when the distance between the nicks was decreased to 46-nt. We have investigated distances smaller than 40-nt between the nicks in PAM-out orientation for Cas9 D10A and found that editing was poor for spacing <35-nt, likely due to steric hindrance between the two RNP molecules (data not shown).

When Cas9 D10A nickase RNP complexes targeting both strands in the PAM-out orientation nick the genomic DNA, a DSB with 5' overhangs is generated. Because both strands are targeted by one of the two gRNAs, there is no canonical 'targeting' and 'non-targeting' strand in nickase experiments; thus, they are referred to as top and bottom strands. The paired-guide double nicking strategy doesn't generate a blunt-ended cut like WT Cas9, so we further explored the possibility of using Cas9 D10A

7

208   to insert exogenous sequences between flanking nick sites at a location that would be otherwise

209   considered sub-optimal for WT Cas9 designs using WT Cas9 and either gRNA on its own. We

210   designed ssODN donor templates for *HPRT1* in which a 6-nt EcoRI restriction enzyme recognition

211   site was introduced at different locations along a donor template (Figure 2A). HDR events mediated

212   by Cas9 D10A in HEK293 cells, as measured by the percentage of EcoRI digestion, ranged from 13-

213   25% across the 51-nt region (Figure 2B, top left panel). In contrast, WT Cas9-mediated HDR

214   decreased dramatically as the intended insertion site moved away from the cleavage site (Figure 2B,

215   top middle and right panels), consistent with our earlier findings. At the position centered between the

216   two cleavage sites (25-nt from left and 26-nt from the right), Cas9 D10A was able to induce a higher

217   HDR insertion frequency than WT Cas9 with either of the individual gRNAs. As a comparison, neither

218   WT Cas9 nor Cas9 H840A with the same gRNA pair demonstrated HDR insertion frequency as high

219   as Cas9 D10A at all positions tested (Supplementary Figure S2C). In addition, at these sites WT

220   Cas9 demonstrated a strong preference for the NT strand donor template (bottom strand for WT with

221   left gRNA, and top strand for WT with right gRNA), especially at positions distant from the cut site,

222   while Cas9 D10A did not show a strand preference. We performed the same experiment in K562

223   cells, which demonstrated robust HDR overall with WT Cas9. As expected, despite both Cas9 D10A

224   and WT Cas9 showing a higher frequency of HDR in this cell line, the ability of Cas9 D10A to mediate

225   higher HDR when moving away from cleavage sites was retained (Figure 2B, bottom panels).

226   In order to verify that the above observations are not site specific, we conducted a similar experiment

227   at a different locus (*AAVS1*, PAM-out design with 46-nt spacing). In addition to 5 insert positions at or

228   between the two cleavage sites, we also included two positions 12-nt upstream or downstream to the

229   left or right cleavage sites, respectively (Supplementary Figure S2D). Consistent with the results

230   described above, Cas9 D10A outperformed WT Cas9 at the position centered between the cleavage

231   sites (position "D") in HEK293 cells (Supplementary Figure S2E). Insertions outside of the nick sites

232   were not as efficient as ones placed between the nick sites. The observation that Cas9 D10A has no

233   identifiable strand preference for the HDR donor template also held true at this site. For HDR

234   experiments with Cas9 D10A, the highest editing efficiency occurred when paired gRNAs were in the

235   PAM-out orientation with the nick sites spaced 40-68 nt apart. Overall, we observed that the desired

236   mutation is best achieved when placed between the two nicks, and we did not observe a consistent

237   strand preference. The use of paired gRNAs with Cas9 D10A nickase allows for HDR insertions at

238   locations not accessible by WT Cas9 nuclease due to design limitations and may be advantageous

239   over WT Cas9 in situations where there is a lack of efficient Cas9 guides near the intended HDR

240   mutation.

241

242   **Optimizing placement and number of blocking mutations with Cas9**

243   Previous studies have demonstrated that incorporating blocking mutations within the donor oligo to

244   prevent re-cleavage by Cas9 nuclease after a desired HDR event improves rates of HDR.[35,45]

245   However, these studies have been limited in the number of constructs tested and have not examined

246   if there is a preference for transversions (e.g. G-to-C purine to pyrimidine conversion), or transitions

247   (e.g. G-to-A purine to purine conversion) in the blocking mutations used. We aimed to further

248   investigate this to define a ruleset for the placement and number of blocking mutation(s) required to

249   maximize HDR efficiency. First, we designed an experiment to determine the effect of a single

250   blocking mutation within the PAM or the seed region of Cas9, which is defined as the PAM-proximal

251   10-12 bases on the 3' end of the guide.[7] Mismatches within the seed region and PAM are known to

252   significantly reduce Cas9 binding and cleavage efficiency, so would be expected to confer the highest

253   reduction in re-cleavage by Cas9.[8,50] Two genomic loci were selected and HDR ssODN donor

254   templates were designed to generate a single base change 3' of the PAM to serve as the desired

255   HDR mutation. This HDR mutation would not impact Cas9 re-cleavage, as it falls outside of the

256   protospacer/PAM sequence. In addition to the desired HDR mutation, a single blocking mutation in

257   the seed region of the guide or PAM was included, where each position tested was changed to every

258   possible alternate base in a unique donor template to determine if any of the four DNA bases are

259   preferred when utilizing blocking mutations (Figure 3A). HDR ssODN donor templates were delivered

260   along with their respective RNP complexes targeting two different genomic loci into HEK293 and

261   K562 cells, and the rate of perfect HDR including both the desired HDR mutation and blocking

262   mutation (where applicable) was assessed by NGS (Figure 3B). As expected, the frequency of the

263   desired HDR mutation ('ctrl') was low, at <2% for all four conditions tested. Adding a blocking

264   mutation in the second or third base of the 'NGG' PAM resulted in the greatest increase, with HDR

265   levels reaching 8.0-17.8%. Blocking mutations placed around the Cas9 cleavage site and near the 3'

266   end of the guide were also highly effective, with the impact reduced as the position of the blocking

267   mutation moved PAM-distal. No base was universally preferred over others in these experiments.

9

268   Next, we aimed to determine if a single blocking mutation was sufficient to prevent re-cleavage of the

269   genomic DNA and maximize the number of HDR events, or if a combination of multiple blocking

270   mutations would lead to higher HDR frequency. Donor templates were designed with a single blocking

271   mutation in the PAM, two blocking mutations in the PAM, and/or blocking mutations at two locations

272   within the seed region. Various combinations of these mutations were delivered as ssODNs along

273   with corresponding RNP complexes targeting four loci in Jurkat cells to assess their ability to mediate

274   a single base change 3' of the PAM via HDR. An example sequence showing the placement of

275   blocking mutation(s) in the donor templates tested is provided in Supplemental Figure 3A. As

276   demonstrated by Supplemental Figure 3B, donor templates containing two blocking mutations led to

277   more robust improvement in HDR efficiency than donor templates containing a single blocking

278   mutation, and this effect was greatest when the blocking mutations were within the PAM or nearer to

279   the 3' end of the guide. Incorporating three or four blocking mutations did not further enhance HDR

280   efficiency over the best combination of 2 blocking mutations (2 PAM or 1 PAM + 1 seed A).

281   We next wanted to investigate this effect when a larger HDR mutation is inserted, such as an EcoRI

282   restriction site, as well as examine the impact of blocking mutations when the HDR insertion was

283   placed at various positions relative to the Cas9 cleavage site. To determine if blocking mutations are

284   beneficial with a 6-nt insertion, we selected four gRNAs and designed donor templates to insert an

285   EcoRI restriction digest recognition site at the Cas9 cleavage site. Donor templates included no

286   blocking mutation (no PAM mutation) or a 'GG' to 'CC' blocking mutation within the PAM sequence

287   (PAM mutation). In addition, donor templates to insert the EcoRI sequence at varying locations

288   relative to the Cas9 cleavage were designed; as a result, these donor templates would facilitate the 6-

289   nt insertion as close as 3-nt from the Cas9 cleavage site and extending as far as 45-nt in both the 5'

290   and 3' direction. Designs of donor templates again contained no blocking mutation or a 'GG' to 'CC'

291   PAM mutation (Supplemental Figure 3C). All donor templates consisted of the NT-strand and

292   maintained homology arms of 40-nt from both the EcoRI insertion location and the Cas9 cut site. The

293   set of 24-32 ssODNs for the four targets were delivered along with their respective Cas9 RNP

294   complex to Jurkat cells by nucleofection (N = 120). Additionally, donor templates and respective Cas9

295   RNP complexes for two of the targets were also delivered to HEK293 cells (N = 48). An EcoRI

296   cleavage assay was used to determine the HDR frequencies, and results are shown in Supplemental

297   Figure 3D. Mutating the PAM from an 'NGG' to 'NCC' increased HDR at locations further from the cut

10

298   site in the 3' direction, downstream of the PAM and outside of the protospacer sequence, where the

299   HDR insertion would not prevent Cas9 re-cleavage. When the EcoRI insertion was within the guide

300   seed region or PAM, incorporating additional PAM mutations negatively impacted the HDR efficiency.

301   This suggests that there is a limit to the number of additional mutations that should be added to

302   prevent Cas9 re-cleavage, and if too many mutations are present the HDR efficiency can be

303   negatively affected.

304   This data represents a subset of HDR donor designs that we tested to fully elucidate a ruleset for the

305   placement and number of blocking mutations required for various HDR mutation types. Using HDR

306   efficiency results from Figure 3B, we generated relative HDR efficiencies (i.e., HDR efficiency with

307   varying blocking mutations divided by HDR efficiency without blocking mutations) and a position

308   specific scoring matrix (PSSM). The PSSM represents the HDR improvement introduced by mutating

309   the HDR donor template at each position along the length of the Cas9 spacer sequence. Using the

310   linear combination PSSM values representing blocking mutations in each HDR donor template, we

311   calculated a blocking score for each of 374 donor template designs associated with 9 guides and

312   delivered into 3 cell lines (HEK293, Jurkat, and Hepa1-6). We generated a model representing a non-

313   linear correlation between blocking scores and HDR efficiency (Figure 3C). A score of 1.97

314   approximately corresponds to mutating both G nucleotides in the Cas9 PAM. The model predicts

315   blocking mutations with scores <1.97 will have a positive impact on HDR rates; while blocking

316   mutations with scores greater than 1.97 have a less certain, and perhaps detrimental, impact.

317   We embedded the PSSM, blocking score model, a guide-to-target mutation model, and other

318   heuristics in the Alt-R HDR Design Tool. The combination of models allows the tool to recommend

319   high quality paired HDR donor templates and guides. In addition, the Alt-R HDR Design Tool uses

320   blocking scores to select block mutations that do not change the protein coding sequence (when

321   transcript information is provided). We tested the Alt-R HDR Design Tool's donor template

322   recommendations using four unique target HDR mutations with or without the addition of silent

323   blocking mutations (Figure 3D), and we delivered the donor templates to HEK293, Hela and Jurkat

324   cells. In every case except one in Jurkat cells, where the HDR rate was unchanged, the donor

325   template designed with the addition of silent mutations yielded higher HDR events than donor

326   template designs without blocking silent mutations (Figure 3E).

327

11

328 **HDR mutation location determines donor strand preference**

329 Achieving efficient HDR at greater distances from the cut site using WT Cas9 to broaden the

330 capabilities of CRISPR genome editing is desirable. We aimed to investigate design considerations

331 for HDR mutations that fall outside of the optimal editing window to determine if there is a donor

332 strand preference. Additionally, we tested if additional mutations along the ssODN repair track, which

333 is defined as the portion of the donor template between the Cas9 cut site and mutation location, were

334 beneficial. We designed ssODN donor templates to create an EcoRI insert 25-nt from the Cas9

335 cleavage site either on the PAM-containing side of the Cas9 cut (PAM-proximal) or on the non-PAM

336 side of the Cas9 cut (PAM-distal) for three genomic loci. Donor templates were designed to have 1)

337 no mutation, 2) an 'NGG' to 'NCC' PAM mutation to prevent re-cleavage after HDR, or 3) mutations

338 placed along the repair track every 5th nt, either alone or in combination with the PAM mutations

339 (Figure 4A). Both the T and NT strands were tested to determine which donor templates facilitated the

340 highest HDR incorporation of an insert outside of the previously established optimal placement.

341 ssODN donor templates were delivered along with their respective Cas9 RNP complexes to HeLa

342 cells by nucleofection, and the frequency of perfect HDR containing both the desired HDR mutation

343 and any additional mutations was determined by NGS. The mean HDR rate for each ssODN design

344 across three biological replicates for each of the three genomic loci tested is shown in Figure 4B (for

345 each ssODN design n = 9). For PAM-distal insertions, the NT strand had an average HDR of 12.7%

346 with repair track mutations compared to 1.6% when the T strand was used. In contrast, for PAM-

347 proximal insertions, the T strand containing repair track and PAM mutations gave higher HDR than

348 the NT strand with the same mutations (8.6% vs 0.8%, respectively). For PAM-proximal insertions, the

349 repair track mutations marginally improved the HDR efficiency above incorporating a PAM mutation

350 alone, increasing the HDR from 7.5% to 8.6%. However, for PAM-distal insertions, the repair track

351 mutations significantly improved the frequency of HDR 3.4-fold over having only a PAM mutation (p

352 <0.01, paired t-test).

353 To further investigate strand preference when HDR mutations are placed at suboptimal distances

354 (>15-nt) away from the Cas9 cleavage site, 12 loci from the set of 254 targets presented in Figure 1B

355 were selected as a subset of gRNAs to carry out this experiment. These gRNAs were selected as

356 sites for HDR because they demonstrated one of three characteristics: no strand preference, an

357 obvious strand preference for the T strand, or an obvious strand preference for the NT strand in either

12

358   Jurkat or HAP1 cells. Donor templates were designed following the same principles as the prior

359   experiment, placing an EcoRI insertion at the Cas9 cleavage site or 20 bases PAM-proximal or PAM-

360   distal. Given the results shown in Figure 4B that identify PAM-distal insertions as mediating sub-

361   optimal insertion frequencies, a single PAM mutation alone was only tested for PAM-proximal

362   insertions. In addition, repair track mutations were incorporated every 3-7 nt between the Cas9

363   cleavage site and the desired HDR mutation (Figure 4C). These ssODN donor templates were

364   delivered to Jurkat and HeLa cells along with their respective Cas9 RNP complexes by nucleofection,

365   and the frequency of perfect HDR was determined by NGS with the mean HDR rate for each ssODN

366   across the 12 genomic loci shown in Figure 4D. Across all 12 sites tested, the NT strand gave higher

367   HDR than the T strand for PAM-distal insertions, and the T strand gave higher HDR than the NT

368   strand for PAM-proximal insertions (Figure 4D, Supplemental Figure 4A). Similar to the previous

369   experiment, repair track mutations in combination with a single PAM mutation for PAM-proximal

370   insertions had a modest improvement in HDR rates over the single PAM mutation alone, increasing

371   from 3.0% to 4.9% in Jurkat cells and 5.4% to 8.7% in Hela cells. The level of HDR improvement for

372   the various mutation strategies had site-to-site variability (Supplemental Figure 4B). However, the

373   strand preference was universal to all sites tested, indicating that for PAM-proximal insertions the T

374   strand should be used as the donor template, and for PAM-distal insertions, the NT strand should be

375   used for the highest rate of HDR.

376

377   **Optimized design rules for HDR with Cas12a**

378   Cas12a is a type II CRISPR-Cas nuclease with several distinct differences to Cas9. Cas12a

379   generates a DSB with 5' overhangs, requires a 'TTTV' PAM, and enables editing in AT-rich

380   genomes.[4] We designed experiments to characterize HDR design rules for Cas12a in a manner

381   similar to what was done with Cas9. First, the optimal placement of an insertion was determined by

382   designing donor templates for five sites in the *HPRT1* gene. These donor templates placed an EcoRI

383   restriction digest recognition site at varying positions relative to the PAM and guide sequence (Figure

384   5A), ranging from 9 bases away in the 5' direction from the first base of the guide to 45 bases 3' of the

385   first base of the guide. The optimal HDR activity for this insert is not centered around the two Cas12a

386   cleavage sites, canonically positioned 18 and 23 bases from the PAM, as was the case for Cas9.

387   There is a strong preference for insertions between positions 12-16 of the guide (Figure 5B).

388   Interestingly, there is an increase in EcoRI insertion around position 24 even though this position falls

389   outside of the protospacer region. We hypothesized this to be a result of imperfect HDR where an

390   EcoRI site is inserted via HDR, followed by Cas12a re-cleavage which then allows the insertion of

391   other indels from NHEJ repair. To investigate this possibility, we performed NGS analysis of one of

392   the five sites from Figure 5B to examine the frequency of perfect HDR insertion relative to imperfect

393   HDR insertion. At position 24, while the amount of EcoRI insertion was 6.4% by EcoRI cleavage

394   (Supplemental Figure 5A), the amount of perfect HDR when measured by NGS is <1% and the

395   imperfect HDR, which includes HDR insertion of an EcoRI site plus subsequent indels from NHEJ due

396   to Cas12a re-cleavage, was 5.9% (Supplemental Figure 5B). Thus, we confirmed by NGS that the

397   optimal position for Cas12a-mediated HDR is between positions 12-16 of the guide and moving an

398   insertion outside of the protospacer can give the desired insertion, but also allows for additional

399   undesired editing.

400   To investigate if Cas12a demonstrates a universal strand preference when an EcoRI insertion was

401   optimally placed, a set of 15 Cas12a guide RNAs was selected and donor templates were designed to

402   insert an EcoRI restriction digest recognition site 16 bases 3' of the PAM. Both the T and NT strand

403   ssODN donor templates were delivered with their respective RNP complexes to Jurkat and HAP1

404   cells by nucleofection, and NGS was used to measure the frequency of total editing and perfect HDR.

405   The combined results from the fifteen sites comparing T and NT strand donors in two cell lines is

406   shown in Figure 5C. Although there are differences in total editing across the 15 sites tested (varying

407   from 30% to >95% total editing which indicates inherent, guide or locus-dependent editing outcomes),

408   universally the total editing was lower when the T strand was used. This is shown in figure 5C, top

409   panel by the data points generally clustering below the line through the origin or showing increased

410   total editing when delivered with the NT strand. The reference line through the origin is included as a

411   benchmark in both panels for 5C to indicate the point at which T strand total editing or HDR is

412   equivalent to NT strand total editing or HDR, respectively. As a result of the discrepancy observed in

413   favor of the NT strand mediating increased total editing (top panel of 5C), the frequency of HDR was

414   also lower when the T strand was used as the donor template than when the NT strand was used.

415   These results demonstrate a statistically significant preference for the use of the NT strand as the

416   donor template to achieve optimal results in HDR experiments using Cas12a nuclease.

14

417   The results from Figure 5B and follow-up in Supplemental Figure 5B suggest that blocking mutations

418   could also be beneficial in Cas12a-mediated HDR. We designed experiments to investigate whether

419   HDR could be improved at a position outside of the guide targeting sequence by incorporating

420   blocking mutations within the ssODN donor template. Donor templates with an EcoRI insertion

421   optimally placed at position 15 of the guide, or sub-optimally at position 24 from the first base of the

422   guide (outside of the guide targeting region) were designed to include no blocking mutation, a

423   blocking mutation of the PAM sequence (TTTV to TVTV), or a blocking mutation within the guide

424   targeting sequence at various positions (Figure 5D). These were tested as NT strand donor templates

425   at two genomic loci within the *HPRT1* gene and in two cell lines, Jurkat and Hela. When the EcoRI

426   cleavage site was inserted within the guide sequence there was no benefit to including blocking

427   mutations to prevent further re-cleavage, likely because the EcoRI site disrupts subsequent cleavage

428   events (Fig 5E, left panel). However, when the EcoRI insertion was outside of the PAM/guide

429   targeting region, blocking mutations increased the rate of HDR from 0.7%, to 13.3% with a mutation in

430   the PAM and 13.0% with a mutation at position 14 of the guide (Figure 5E, right panel). These results

431   show that, similar to Cas9, blocking mutations are beneficial with Cas12a and can be used to broaden

432   the available window for efficient HDR insertions.

433

434   **Alt-R modified HDR Donor oligos and Alt-R HDR Enhancer reagents further improve HDR**

435   It has been previously reported that the addition of phosphorothioate (PS) modifications improve HDR

436   efficiency.[39,46] We investigated over 20 different stabilizing modifications (data not shown) and have

437   developed Alt-R HDR Donor Oligos which include 2 PS linkages at the ultimate and penultimate

438   backbone linkage and an end-blocking modification at both the 5' and 3' end to provide increased

439   stability. We designed 7 donor templates to insert a 6-nt EcoRI site with 30 to 40-nt homology arms at

440   unique genomic loci, and 1 donor template designed to insert a 42-nt sequence with 60-nt homology

441   arms. These contained either no modification (unmodified), two PS linkages at each end of the donor

442   template (PS modified) or Alt-R modified donor templates. They were delivered to HeLa cells by

443   nucleofection along with corresponding RNP complexes consisting of sgRNAs complexed with Alt-R

444   *S.p.* HiFi Cas9 nuclease. PS modified donor templates confer improved HDR over unmodified donor

445   templates, with an average of 3.1-fold improvement (Figure 6A). Alt-R modifications provided further

15

446   increase in HDR over both unmodified and PS modified donor templates by an average of 5.2-fold

447   and 1.7-fold, respectively.

448   Another strategy to increase HDR is to add chemical compounds that inhibit NHEJ repair and

449   promote HDR repair.[47-49] We tested two commercially available compounds, Alt-R HDR Enhancer V1

450   and Alt-R HDR Enhancer V2, for their ability to promote HDR. Four genomic loci for Cas9 and four

451   genomic loci for Cas12a were selected and Alt-R modified donor templates containing 40-nt

452   homology arms were designed to insert an EcoRI cleavage site at the optimal position (at the Cas9

453   cleavage site or at position 16 of the Cas12a guide). After standard delivery of ssODNs with gRNAs

454   via lipofection (HEK293-Cas9 cells, which stably express Cas9 nuclease) or ssODNs with RNP

455   complexes by nucleofection (K562, Jurkat) cells were plated in media containing HDR Enhancer V1,

456   HDR Enhancer V2, DMSO, or untreated (data not shown), with a media change after 24 hours to

457   standard media. With Cas9, HDR Enhancer V1 increased HDR frequencies by 1.5-, 1.6-, and 2.1-fold

458   in HEK293-Cas9, K562, and Jurkat cells, respectively. With Cas12a delivery, HDR Enhancer V1

459   increased HDR frequencies 1.6, and 1.1-fold in K562 and Jurkat cells, respectively. With Cas9, HDR

460   Enhancer V2 increased HDR frequencies 2.2-, 1.9-, and 3.2-fold in HEK293-Cas9, K562, and Jurkat

461   cells, respectively. With Cas12a delivery, HDR Enhancer V2 increased HDR frequencies 1.7- and 1.9-

462   fold in K562 and Jurkat cells, respectively (Figure 6B).

463   Finally, we investigated if the use Alt-R HDR Enhancer V1 in combination with modified donor

464   templates improved HDR further than if just one of these reagents was used. In this experiment Alt-R

465   HDR Enhancer V1 was used, although we have observed similar results with Alt-R HDR Enhancer V2

466   (data not shown). We found that the maximal HDR efficiency was achieved when Alt-R modified HDR

467   donor templates were used and cells were incubated with Alt-R HDR Enhancer V1 (Figure 6C). The

468   donor templates targeting *HPRT1* had 5.9% HDR using an unmodified DNA donor template, which

469   was increased 4.8-fold to 28.4% using an Alt-R modified donor template. The addition of Alt-R HDR

470   Enhancer V1 further increased the frequency of HDR 1.8-fold to 52.0%. Similarly, HDR at the *MYC*

471   locus increased from 15% HDR using an unmodified donor template to 57.5% HDR with the

472   combined use of an Alt-R modified donor template and Alt-R HDR Enhancer V1. The same was true

473   for *SAA1*, which had HDR frequency of 4.1% with an unmodified donor template, 18.5% with an Alt-R

474   modified donor template, and 39.4% HDR with the combination of Alt-R modified donor template and

475   Alt-R HDR Enhancer V1, an overall increase of 9.6-fold.

476

477 **DISCUSSION**

478 ssODN donor templates are routinely used to generate mutations or small insertions with CRISPR-

479 Cas proteins. This is desirable for many applications including the generation of functional domains

480 such as epitope tags or fluorescent proteins fused to endogenous genes for biological studies,

481 creation of cell lines with a known mutation for disease modeling, and correction of a genetic disease

482 for therapeutic applications.[36,51,52] However, the design of these donor templates remains challenging

483 for researchers due to uncertainty about which CRISPR-Cas system should be applied, selection of

484 gRNA(s) for each new HDR mutation location, and which donor template strand should be used to

485 achieve the highest frequency of HDR. In addition, the design process for ssODN donors can be time-

486 consuming, particularly if the researcher wishes to add silent blocking mutations to prevent re-

487 cleavage and maintain amino acid translation. We have thoroughly investigated design considerations

488 for *S.p.* Cas9 nuclease, *S.p.* Cas9 D10A nickase and *A.s.* Cas12a nuclease and present optimized

489 design considerations for each enzyme, including positioning of the gRNA(s) relative to the desired

490 mutation, donor strand preference, and the incorporation of blocking mutations to improve desired

491 HDR. Additionally, we have identified donor template chemical modifications and small molecule

492 compounds that further increase rates of HDR.

493 When starting an HDR genome editing project the first consideration is which CRISPR-Cas enzyme to

494 utilize. Our results support that this choice should be dependent on where the relative genomic

495 location of the desired mutation(s) resides in relation to the available CRISPR-Cas guides. If there is

496 an 'NGG' PAM near the desired mutation (<15 bases), and this guide is expected or known to edit

497 efficiently, then WT Cas9 can be used with confidence. If the available 'NGG' PAM sites are greater

498 than 15 bases from the desired mutation, then the use of a PAM-out paired guide design with Cas9

499 D10A nickase may confer higher HDR than WT Cas9, provided the mutation is placed between the

500 two nick sites generated by Cas9 D10A. This can be particularly useful if additional blocking

501 mutations are not desired or off-target DSBs are a concern. Alternatively, if there is a 'TTTV' PAM site

502 that is positioned so the HDR mutation lies between the 12-16th bases of a Cas12a protospacer, then

503 Cas12a is a viable option, although, like *S.p.* Cas9, this window can be extended with the

504 incorporation of blocking mutations. When multiple gRNA options are available for a desired HDR

17

505   edit, screening several may help eliminate any low activity guides to determine which will yield the

506   highest HDR.

507   The availability of efficient Cas9 guides near a desired mutation is a significant limitation for many

508   HDR experiments. In many cases, the guide or guides closest to the desired HDR mutation are sub-

509   optimal in terms of cleavage efficiency or proximity. While using a paired-guide nickase strategy is

510   viable, the requirement of having two guides with optimal spacing, activity, and orientation limits the

511   design options and precludes this strategy for certain sites where there are no nickase designs

512   available. Paix et al.[44] demonstrated that incorporating additional mutations in the repair track

513   between the cut site and desired HDR mutation location facilitated a wider region of donor integration.

514   We observed this to be beneficial for PAM-distal HDR events. However, repair track mutations in

515   combination with PAM mutations did not yield the highest HDR. This is likely because the repair track

516   mutations were sufficient to prevent Cas9 re-cleavage without additional mutations in the PAM and

517   the PAM mutation is on the opposite side of the Cas9 cleavage event, which may fall outside of the

518   effective conversion zone for SDSA repair.[38] For PAM-proximal HDR mutations, repair track mutations

519   were beneficial for some sites, but not all, indicating that this strategy is effective in certain cases. In

520   situations where optimally spaced Cas9 or Cas12a guide designs are not possible, incorporating

521   mutations within the repair track between the cut site and desired HDR mutation or within the PAM

522   may improve the rate of successful HDR.

523   The addition of blocking mutations has been demonstrated to improve HDR depending on the

524   selected guide RNA and its relative positioning to the desired HDR mutation. Blocking mutations are

525   beneficial when the desired HDR mutation does not prevent re-cleavage by the CRISPR-Cas

526   nuclease. We have optimized the design of blocking mutations for use with Cas9 nuclease, including

527   the placement and number of blocking mutations required, and this has been built into the Alt-R HDR

528   Design Tool which facilitates simple donor template design in an easy to navigate interface. The Alt-R

529   HDR Design Tool allows for gRNA selection for both WT Cas9, balancing the distance from the cut to

530   mutation and on- and off-target scores of available gRNAs, and Cas9 D10A nickase, where the gRNA

531   orientation and distance between nick sites is considered. In addition, the Alt-R HDR Design Tool

532   provides the option to add silent blocking mutations using our empirically defined ruleset. In our study,

533   we identified no bias in which alternate base was used as the blocking mutation to prevent Cas9 re-

534   cleavage, indicating that there is flexibility in designing appropriate silent blocking mutations so as to

18

535   not affect coding sequence. However, this could also indicate that the effect size is small or site-

536   specific and with a larger data set potential differences between alternate bases used for silent

537   blocking mutations could be resolved. Further investigation into the optimized number and placement

538   of blocking mutations with Cas12a is underway with the expectation that this will be built into a tool for

539   Cas12a HDR donor template design.

540   After a CRISPR-Cas system and gRNA(s) have been selected and the donor template has been

541   designed, the next consideration for HDR experiments is the selection of homology arm lengths. In

542   previous work investigating HDR improvements in the cell lines mentioned above, asymmetric

543   homology arms did not improve HDR beyond symmetric homology arms when arm length was ≥30-nt

544   from both the mutation location and the Cas9 cleavage site (data not shown). As such, the standard

545   approach we employ is to design ssODN donor templates with 40-nt homology arms. The Alt-R HDR

546   Design Tool allows for custom homology arm lengths to accommodate asymmetric designs, if desired.

547   A final donor template design consideration that we investigated was strand preference for the donor

548   template. Cas9 D10A nickase did not demonstrate a strong strand preference, so testing both strands

549   to determine which results in the highest HDR frequency may be prudent. However, for WT Cas9 the

550   preferred strand is strongly dependent upon where the desired HDR mutation is, relative to the Cas9

551   gRNA. Previous reports have demonstrated that when using ssODN donor templates with Cas9

552   nuclease the SDSA mechanism of repair is preferentially utilized, which consists of two steps.[38] After

553   a DSB is generated, the ends are resected, generating 3' overhangs which are then available for base

554   pairing with the donor DNA. This donor DNA then serves as a template for 5' to 3' DNA synthesis.

555   Although we observed no universal donor strand preference in the experiment outlined in Figure 1B,

556   the HDR insertion was placed directly at the Cas9 cleavage site where the SDSA model predicts high

557   relative HDR regardless of the donor strand used. However, for insertions further from the Cas9

558   cleavage site there is a preference for the donor strand that contains 3' sequence complementary to

559   the overhangs generated during DSB repair.[44] For PAM-proximal insertions the T strand should be

560   used, and for PAM-distal mutations the NT strand should be used, consistent with the SDSA model of

561   DSB repair using ssODN donor templates. For mutations directly at the cut site, we provide some

562   evidence that the use of the T strand may reduce total editing with Cas9 which negatively impacts

563   HDR, but this was not the case for both cell types tested. Using Cas12a, we observed a reduction in

564   total editing rates when the T strand was used universally. We hypothesize that the donor template

19

565   acts as a sponge for RNP, reducing the concentration available for genome editing within cells, or

566   activates the non-specific ssDNase activity of Cas12a. The NT strand conferred increased HDR for

567   experiments with Cas12a over the T strand. However, the effect of HDR insertion placement has not

568   been thoroughly investigated for Cas12a to determine if the T strand will be advantageous over the

569   NT strand for PAM-proximal mutations in a manner similar to Cas9 and further experimentation is

570   required.

571   Beyond donor template design considerations, the use of optimized reagents for HDR experiments

572   can further improve the frequency of HDR-mediated repair. The use of end-protecting modifications to

573   stabilize ssODN donor templates within the cellular environment has been demonstrated to improve

574   HDR rates, and we have developed a novel end-blocking modification that confers the highest level of

575   improvement over unmodified DNA templates, compared to previously reported constructs. Further,

576   we have identified two small molecules that can be used to inhibit the NHEJ pathway to improve HDR

577   over untreated cells. We have demonstrated that when incorporated into our workflows these

578   compounds improve HDR up to 3.2-fold in immortalized cell lines and function in combination with

579   modified donor templates to provide further improvements in HDR frequencies. We have studied

580   design rules for *A.s.* Cas12a nuclease, which had not yet been systematically examined. Further, the

581   ruleset for *S.p.* Cas9 and *S.p.* Cas9 D10A nickase have been incorporated into a novel bioinformatic

582   tool for HDR donor template design. Taken altogether, these findings present design

583   recommendations and optimized reagents for achieving high frequency of precise repair outcomes

584   utilizing HDR in mammalian cell lines.

585

586   **METHODS**

587   **Ribonucleoprotein complex formation**

588   Cas9 gRNAs were prepared by mixing equimolar amounts of Alt-R™ crRNA and Alt-R tracrRNA

589   (Integrated DNA Technologies, Coralville, IA, USA) in IDT Duplex Buffer (30 mM HEPES, pH 7.5, 100

590   mM potassium acetate; Integrated DNA Technologies), heating to 95°C and slowly cooling to room

591   temperature or using Alt-R sgRNA (Integrated DNA Technologies) hydrated in IDTE pH 7.5 (10 mM

592   Tris, pH 7.5, 0.1 mM EDTA; Integrated DNA Technologies). Cas12a gRNAs consisted of Alt-R

593   Cas12a crRNAs (Integrated DNA Technologies) hydrated in IDTE pH 7.5. RNP complexes were

594   assembled by combining the CRISPR-Cas nuclease (Alt-R *S.p.* Cas9 Nuclease V3, Alt-R *S.p.* HiFi

20

595   Cas9 Nuclease V3, Alt-R *S.p.* Cas9 D10A V3, Alt-R *S.p.* Cas9 H840A V3, Alt-R *A.s.* Cas12a V3, or

596   Alt-R *A.s.* Cas12a *Ultra*; Integrated DNA Technologies) and the Alt-R gRNA at a 1:1 to 1.2:1 molar

597   ratio of gRNA:protein and incubating at room temperature for 30 minutes. For paired nicking

598   experiments, each RNP was formed separately, and two RNPs were mixed together at an equal

599   molar ratio prior to adding to the cells at the time of transfection. The 20-nt target specific sequences

600   of the gRNAs used in this study are listed in Supplementary Table 1.

601

602   **HDR ssODN donor templates**

603   Alt-R™ HDR Donor Oligos (Integrated DNA Technologies) used in this study consisted of either Alt-R

604   modified (containing two phosphorothioate linkages at the ultimate and penultimate backbone linkage

605   and an IDT proprietary end-blocking modification at 5' and 3' ends), PS modified (containing two

606   phosphorothioate linkages at the ultimate and penultimate backbone linkage at 5' and 3' ends) or

607   unmodified DNA. Donor oligos were hydrated using IDTE pH 7.5 (Integrated DNA Technologies).

608   Sequences of the HDR oligos used in this study are listed in Supplementary Table 1.

609

610   **Cell culture**

611   HAP1, HEK293, HeLa, Jurkat E6-1, and K562 cells were purchased from ATCC® (Manassas, VA,

612   USA), and maintained in DMEM (HEK293, and HeLa), RPMI-1640 (Jurkat) and IMDM (HAP1, K562)

613   (ATCC), each supplemented with 10% fetal bovine serum (FBS) and 1% penicillin-streptomycin

614   (Thermo Fisher Scientific, Carlsbad, CA, USA). HEK293 cells that constitutively express Cas9

615   nuclease ("HEK293-Cas9") were generated by stable integration of a human-codon optimized *S.p.*

616   Cas9 as well as the flanking 5' and 3' nuclear localizing sequences and 5'-V5 tag from the GeneArt

617   CRISPR Nuclease Vector (Thermo Fisher Scientific). HEK293-Cas9 cells were maintained in DMEM

618   supplemented with 10% FBS, 1% penicillin-streptomycin, and 500 µg/mL G418 (Thermo Fisher

619   Scientific). Cells were incubated at 37°C with 5% CO_2 and passaged every 3 days. HAP1 cells were

620   used for transfection at 50-70% confluency. HEK293 and HeLa cells were used for transfection at 70-

621   90% confluency. Jurkat and K562 were used for transfection at 5-8 x 10^5 cells/mL density. After

622   transfection, cells were grown for 48-72 hours in total, after which genomic DNA was isolated using

623   QuickExtract™ DNA Extraction Solution (Epicentre, Madison, WI, USA).

624

625 **Delivery of genome editing reagents by lipofection**

626 Lipofection was performed in 96-well plates. First, 25 µL of Opti-MEM® (Thermo Fisher Scientific)

627 containing 1.2 µL (RNP delivery) or 0.75 µL (gRNA delivery) of Lipofectamine® RNAiMAX (Thermo

628 Fisher Scientific) was combined with equal volume of Opti-MEM containing RNP or gRNA and HDR

629 donor template (when present), and incubated at room temperature for 20 min. After lipoplex

630 formation, 4.5×10^4 cells resuspended in 100 µL of DMEM + 10% FBS were added to the transfection

631 complex which resulted in a final concentration of 10 nM RNP or gRNA and 3 nM HDR oligo on a per-

632 well basis. Transfection plates were incubated at 37°C and 5% CO_2.

633

634 **Delivery of genome editing reagents by nucleofection**

635 Electroporation was performed using the Lonza™ Nucleofector™ 96-well Shuttle™ System (Lonza,

636 Basel, Switzerland). For each nucleofection, cells were washed with 1X phosphate buffered saline

637 (PBS) and resuspended in 20 µL of solution SF or SE (Lonza). Cell suspensions were combined with

638 RNP complex(es), Alt-R Cas9 or Cpf1 (Cas12a) Electroporation Enhancer (Integrated DNA

639 Technologies) and HDR donor template (if applicable). This mixture was transferred into one well of a

640 Nucleocuvette™ Plate (Lonza) and electroporated using manufacturer's recommended protocols

641 (except for HEK293, which used protocol 96-DS-150). After nucleofection, 75 µL pre-warmed culture

642 media was added to the cell mixture in the cuvette, mixed by pipetting, and 25 µL was transferred to a

643 96-well culture plate with 175 µL pre-warmed culture media. Transfection plates were incubated at

644 37°C and 5% CO_2.

645

646 **Addition of Alt-R HDR Enhancer**

647 For experiments using HDR Enhancer, cells were transfected as described. Immediately following

648 transfection, cells were grown in media containing either DMSO as a vehicle control, Alt-R™ HDR

649 Enhancer V1 at a final concentration of 30 µM, or Alt-R HDR Enhancer V2 at a final concentration of 1

650 µM. 24 hours after transfection, media was aspirated away without disturbing the cells and fresh

651 media was added to each well.

652

653 **T7 Endonuclease I (T7EI) Assay and restriction enzyme digestion**

22

654   Genomic DNA was extracted after 48-72 hrs incubation using 50 µL Quick Extract™ DNA Extraction

655   Solution (Lucigen, Middleton, WI, USA) following the manufacturer's protocol. Genomic DNA was

656   diluted 3-fold with nuclease-free water and 1.5 µL was PCR-amplified using 0.15 U KAPA HiFi

657   HotStart DNA Polymerase (Kapa Biosystems, Wilmington, MA, USA) in a final volume of 10 µL. For

658   HDR analysis using restriction enzyme digestion, 10 µL of the PCR product was incubated with 2 U of

659   EcoRI-HF® in 1X CutSmart® Buffer (New England BioLabs, Ipswich, MA, USA) at 37°C for 60

660   minutes. Total editing rate was measured using the Alt-R™ Genome Editing Detection Kit (T7EI)

661   (Integrated DNA Technologies) following the manufacturer's protocol. Cleavage products were

662   separated on the Fragment Analyzer™ using the CRISPR Mutation Discovery Kit (Agilent

663   Technologies, Santa Clara, CA, USA). Editing and HDR frequencies were calculated using the

664   following formula: average molar concentration of the cut products / (average molar concentration of

665   the cut products + molar concentration of the uncut product) x 100. PCR primers are listed in

666   Supplementary Table 1.

667

668   **Quantification of editing events by next-generation sequencing (NGS)**

669   On-target editing and HDR efficiencies were also measured by NGS. Libraries were prepared using

670   an amplification-based method as described previously [53]. In short, the first round of PCR was

671   performed using target specific primers, and the second round of PCR incorporates P5 and P7

672   Illumina adapters to the ends of the amplicons for universal amplification. Libraries were purified using

673   Agencourt® AMPure® XP system (Beckman Coulter, Brea, CA, USA), and quantified with qPCR

674   before loading onto the Illumina® MiSeq platform (Illumina, San Diego, CA, USA). Paired end, 150 bp

675   reads were sequenced using V2 chemistry. Data were analyzed using a custom-built pipeline. Data

676   was demultiplexed using Picard tools v2.9 (https://github.com/broadinstitute/picard). Forward and

677   reverse reads were merged into extended amplicons (flash v1.2.11)[54] before being aligned against

678   the GRCh38 genomic reference (minimap2 v2.12).[55] Reads were aligned to the target, favoring

679   alignment choices with indels near the predicted cut site(s). At each target, editing was calculated as

680   the percentage of total reads containing an indel within an 8bp window of the cut site for Cas9 or a

681   9bp window from the -3 position of the Cas12a PAM distal cut site. PCR primers are listed in

682   Supplementary Table 1.

683

23

684 **Statistical Analysis**

685 The data collected from experiments were analysed on Graph PadPrism 8 using two-tailed unpaired t-

686 test to evaluate significance (*$p < 0.05$, **$p < 0.01$, ***$p < 0.001$, and ****$p < 0.0001$).

687

688 **DATA AVAILABILITY**

689 The Alt-R HDR Design Tool is a free online tool that is available from the Integrated DNA

690 Technologies website (https://www.idtdna.com/pages/tools/alt-r-crispr-hdr-design-tool). NGS data

691 used for the figures and supplementary figures have been made available at SRA BioProject

692 Accession # PRJNA638623.

693

694 **ACKNOWLEDGEMENTS**

699

700 **AUTHOR CONTRIBUTIONS**

701 Conceptualization, M.S.S, B.T., J.W., R.T., S.Y., M.S.M. and G.R.R; Software, G.K. and M.S.M.;

702 Investigation, M.S.S., B.T., J.W., R.T. and S.Y.; Data Curation, M.S.S. and M.S.M.; Writing-Original

703 Draft, M.S.S.; Writing-Review & Editing, M.S.S., B.T., J.W., R.T., S.Y., G.K., M.S.M. and G.R.R.;

704 Supervision: G.R.R.

705

706 **REFERENCES**

707 1   Cong, L. *et al.* Multiplex genome engineering using CRISPR/Cas systems. *Science* **339**, 819-

708   823, doi:10.1126/science.1231143 (2013).

709 2   Mali, P. *et al.* RNA-guided human genome engineering via Cas9. *Science* **339**, 823-826,

710   doi:10.1126/science.1232033 (2013).

711 3   Wang, H., La Russa, M. & Qi, L. S. CRISPR/Cas9 in Genome Editing and Beyond. *Annual review*

712   *of biochemistry* **85**, 227-264, doi:10.1146/annurev-biochem-060815-014607 (2016).

24

713   4   Zetsche, B. *et al.* Cpf1 is a single RNA-guided endonuclease of a class 2 CRISPR-Cas system.

714   *Cell* **163**, 759-771, doi:10.1016/j.cell.2015.09.038 (2015).

715   5   Hur, J. K. *et al.* Targeted mutagenesis in mice by electroporation of Cpf1 ribonucleoproteins.

716   *Nature biotechnology*, doi:10.1038/nbt.3596 (2016).

717   6   Deltcheva, E. *et al.* CRISPR RNA maturation by trans-encoded small RNA and host factor

718   RNase III. *Nature* **471**, 602-607, doi:10.1038/nature09886 (2011).

719   7   Jinek, M. *et al.* A programmable dual-RNA-guided DNA endonuclease in adaptive bacterial

720   immunity. *Science* **337**, 816-821, doi:10.1126/science.1225829 (2012).

721   8   Jiang, F. & Doudna, J. A. CRISPR-Cas9 Structures and Mechanisms. *Annu Rev Biophys* **46**, 505-

722   529, doi:10.1146/annurev-biophys-062215-010822 (2017).

723   9   Kim, S., Kim, D., Cho, S. W., Kim, J. & Kim, J. S. Highly efficient RNA-guided genome editing in

724   human cells via delivery of purified Cas9 ribonucleoproteins. *Genome research* **24**, 1012-

725   1019, doi:10.1101/gr.171322.113 (2014).

726   10   Anders, C. & Jinek, M. In vitro enzymology of Cas9. *Methods in enzymology* **546**, 1-20,

727   doi:10.1016/B978-0-12-801185-0.00001-5 (2014).

728   11   Liang, X. *et al.* Rapid and highly efficient mammalian cell engineering via Cas9 protein

729   transfection. *Journal of biotechnology* **208**, 44-53, doi:10.1016/j.jbiotec.2015.04.024 (2015).

730   12   Liang, Z. *et al.* Efficient DNA-free genome editing of bread wheat using CRISPR/Cas9

731   ribonucleoprotein complexes. *Nat Commun* **8**, 14261, doi:10.1038/ncomms14261 (2017).

732   13   Hendel, A. *et al.* Chemically modified guide RNAs enhance CRISPR-Cas genome editing in

733   human primary cells. *Nature biotechnology* **33**, 985-989, doi:10.1038/nbt.3290 (2015).

734   14   Mekler, V., Minakhin, L., Semenova, E., Kuznedelov, K. & Severinov, K. Kinetics of the CRISPR-

735   Cas9 effector complex assembly and the role of 3'-terminal segment of guide RNA. *Nucleic*

736   *Acids Res* **44**, 2837-2845, doi:10.1093/nar/gkw138 (2016).

25

737 15 Davis, L. & Maizels, N. Homology-directed repair of DNA nicks via pathways distinct from

738   canonical double-strand break repair. *Proc Natl Acad Sci U S A* **111**, E924-932,

739   doi:10.1073/pnas.1400236111 (2014).

740 16 Chen, X. *et al.* In trans paired nicking triggers seamless genome editing without double-

741   stranded DNA cutting. *Nat Commun* **8**, 657, doi:10.1038/s41467-017-00687-1 (2017).

742 17 Ran, F. A. *et al.* Double nicking by RNA-guided CRISPR Cas9 for enhanced genome editing

743   specificity. *Cell* **154**, 1380-1389, doi:10.1016/j.cell.2013.08.021 (2013).

744 18 Kocher, T. *et al.* Cut and Paste: Efficient Homology-Directed Repair of a Dominant Negative

745   KRT14 Mutation via CRISPR/Cas9 Nickases. *Mol Ther* **25**, 2585-2598,

746   doi:10.1016/j.ymthe.2017.08.015 (2017).

747 19 Cho, S. W. *et al.* Analysis of off-target effects of CRISPR/Cas-derived RNA-guided

748   endonucleases and nickases. *Genome research* **24**, 132-141, doi:10.1101/gr.162339.113

749   (2014).

750 20 Bothmer, A. *et al.* Characterization of the interplay between DNA repair and CRISPR/Cas9-

751   induced DNA lesions at an endogenous locus. *Nat Commun* **8**, 13905,

752   doi:10.1038/ncomms13905 (2017).

753 21 Shen, B. *et al.* Efficient genome modification by CRISPR-Cas9 nickase with minimal off-target

754   effects. *Nature methods* **11**, 399-402, doi:10.1038/nmeth.2857 (2014).

755 22 Fauser, F., Schiml, S. & Puchta, H. Both CRISPR/Cas-based nucleases and nickases can be

756   used efficiently for genome engineering in Arabidopsis thaliana. *Plant J* **79**, 348-359,

757   doi:10.1111/tpj.12554 (2014).

758 23 Satomura, A. *et al.* Precise genome-wide base editing by the CRISPR Nickase system in yeast.

759   *Sci Rep* **7**, 2095, doi:10.1038/s41598-017-02013-7 (2017).

760 24 Xu, T. *et al.* Efficient Genome Editing in Clostridium cellulolyticum via CRISPR-Cas9 Nickase.

761   *Appl Environ Microbiol* **81**, 4423-4431, doi:10.1128/AEM.00873-15 (2015).

26

762   25   Schiml, S., Fauser, F. & Puchta, H. The CRISPR/Cas system can be used as nuclease for in

763   planta gene targeting and as paired nickases for directed mutagenesis in Arabidopsis

764   resulting in heritable progeny. *Plant J* **80**, 1139-1150, doi:10.1111/tpj.12704 (2014).

765   26   Mikami, M., Toki, S. & Endo, M. Precision Targeted Mutagenesis via Cas9 Paired Nickases in

766   Rice. *Plant Cell Physiol* **57**, 1058-1068, doi:10.1093/pcp/pcw049 (2016).

767   27   Tsai, S. Q. *et al.* GUIDE-seq enables genome-wide profiling of off-target cleavage by CRISPR-

768   Cas nucleases. *Nature biotechnology* **33**, 187-197, doi:10.1038/nbt.3117 (2015).

769   28   Kim, D. *et al.* Genome-wide analysis reveals specificities of Cpf1 endonucleases in human

770   cells. *Nature biotechnology*, doi:10.1038/nbt.3609 (2016).

771   29   Chen, J. S. *et al.* CRISPR-Cas12a target binding unleashes indiscriminate single-stranded

772   DNase activity. *Science* **360**, 436-439, doi:10.1126/science.aar6245 (2018).

773   30   Rouet, P., Smih, F. & Jasin, M. Introduction of double-strand breaks into the genome of

774   mouse cells by expression of a rare-cutting endonuclease. *Mol Cell Biol* **14**, 8096-8106

775   (1994).

776   31   Carroll, D. Genome engineering with targetable nucleases. *Annual review of biochemistry* **83**,

777   409-439, doi:10.1146/annurev-biochem-060713-035418 (2014).

778   32   van Overbeek, M. *et al.* DNA Repair Profiling Reveals Nonrandom Outcomes at Cas9-

779   Mediated Breaks. *Molecular cell* **63**, 633-646, doi:10.1016/j.molcel.2016.06.037 (2016).

780   33   Mao, Z., Bozzella, M., Seluanov, A. & Gorbunova, V. Comparison of nonhomologous end

781   joining and homologous recombination in human cells. *DNA Repair (Amst)* **7**, 1765-1771,

782   doi:10.1016/j.dnarep.2008.06.018 (2008).

783   34   Chen, F. *et al.* High-frequency genome editing using ssDNA oligonucleotides with zinc-finger

784   nucleases. *Nature methods* **8**, 753-755, doi:10.1038/nmeth.1653 (2011).

785   35   Paquet, D. *et al.* Efficient introduction of specific homozygous and heterozygous mutations

786   using CRISPR/Cas9. *Nature* **533**, 125-129, doi:10.1038/nature17664 (2016).

787   36   Skarnes, W. C., Pellegrino, E. & McDonough, J. A. Improving homology-directed repair

788   efficiency in human stem cells. *Methods* **164-165**, 18-28, doi:10.1016/j.ymeth.2019.06.016

789   (2019).

790   37   Wang, Y. *et al.* Systematic evaluation of CRISPR-Cas systems reveals design principles for

791   genome editing in human cells. *Genome biology* **19**, 62, doi:10.1186/s13059-018-1445-x

792   (2018).

793   38   Kan, Y., Ruis, B., Takasugi, T. & Hendrickson, E. A. Mechanisms of precise genome editing

794   using oligonucleotide donors. *Genome research* **27**, 1099-1111, doi:10.1101/gr.214775.116

795   (2017).

796   39   Liang, X., Potter, J., Kumar, S., Ravinder, N. & Chesnut, J. D. Enhanced CRISPR/Cas9-mediated

797   precise genome editing by improved design and delivery of gRNA, Cas9 nuclease, and donor

798   DNA. *Journal of biotechnology* **241**, 136-146, doi:10.1016/j.jbiotec.2016.11.011 (2017).

799   40   Richardson, C. D., Ray, G. J., DeWitt, M. A., Curie, G. L. & Corn, J. E. Enhancing homology-

800   directed genome editing by catalytically active and inactive CRISPR-Cas9 using asymmetric

801   donor DNA. *Nature biotechnology* **34**, 339-344, doi:10.1038/nbt.3481 (2016).

802   41   O'Brien, A. R., Wilson, L. O. W., Burgio, G. & Bauer, D. C. Unlocking HDR-mediated nucleotide

803   editing by identifying high-efficiency target sites using machine learning. *Scientific reports* **9**,

804   2788, doi:10.1038/s41598-019-39142-0 (2019).

805   42   Yang, L. *et al.* Optimization of scarless human stem cell genome editing. *Nucleic acids*

806   *research* **41**, 9049-9061, doi:10.1093/nar/gkt555 (2013).

807   43   Bialk, P., Rivera-Torres, N., Strouse, B. & Kmiec, E. B. Regulation of Gene Editing Activity

808   Directed by Single-Stranded Oligonucleotides and CRISPR/Cas9 Systems. *PloS one* **10**,

809   e0129308, doi:10.1371/journal.pone.0129308 (2015).

28

810   44   Paix, A. *et al.* Precision genome editing using synthesis-dependent repair of Cas9-induced

811   DNA breaks. *Proceedings of the National Academy of Sciences of the United States of*

812   *America* **114**, E10745-E10754, doi:10.1073/pnas.1711979114 (2017).

813   45   Okamoto, S., Amaishi, Y., Maki, I., Enoki, T. & Mineno, J. Highly efficient genome editing for

814   single-base substitutions using optimized ssODNs with Cas9-RNPs. *Scientific reports* **9**, 4811,

815   doi:10.1038/s41598-019-41121-4 (2019).

816   46   Renaud, J. B. *et al.* Improved Genome Editing Efficiency and Flexibility Using Modified

817   Oligonucleotides with TALEN and CRISPR-Cas9 Nucleases. *Cell reports* **14**, 2263-2272,

818   doi:10.1016/j.celrep.2016.02.018 (2016).

819   47   Maruyama, T. *et al.* Increasing the efficiency of precise genome editing with CRISPR-Cas9 by

820   inhibition of nonhomologous end joining. *Nature biotechnology* **33**, 538-542,

821   doi:10.1038/nbt.3190 (2015).

822   48   Riesenberg, S. & Maricic, T. Targeting repair pathways with small molecules increases

823   precise genome editing in pluripotent stem cells. *Nature communications* **9**, 2164,

824   doi:10.1038/s41467-018-04609-7 (2018).

825   49   Ma, X. *et al.* Small molecules promote CRISPR-Cpf1-mediated genome editing in human

826   pluripotent stem cells. *Nature communications* **9**, 1303, doi:10.1038/s41467-018-03760-5

827   (2018).

828   50   Pattanayak, V. *et al.* High-throughput profiling of off-target DNA cleavage reveals RNA-

829   programmed Cas9 nuclease specificity. *Nature biotechnology* **31**, 839-843,

830   doi:10.1038/nbt.2673 (2013).

831   51   Antony, J. S. *et al.* Gene correction of HBB mutations in CD34(+) hematopoietic stem cells

832   using Cas9 mRNA and ssODN donors. *Mol Cell Pediatr* **5**, 9, doi:10.1186/s40348-018-0086-1

833   (2018).

834   52   Dewari, P. S. *et al.* An efficient and scalable pipeline for epitope tagging in mammalian stem

835   cells using Cas9 ribonucleoprotein. *eLife* **7**, doi:10.7554/eLife.35069 (2018).

836   53   Jacobi, A. M. *et al.* Simplified CRISPR tools for efficient genome editing and streamlined

837   protocols for their delivery into mammalian cells and mouse zygotes. *Methods* **121-122**, 16-

838   28, doi:10.1016/j.ymeth.2017.03.021 (2017).

839   54   Magoc, T. & Salzberg, S. L. FLASH: fast length adjustment of short reads to improve genome

840   assemblies. *Bioinformatics* **27**, 2957-2963, doi:10.1093/bioinformatics/btr507 (2011).

841   55   Li, H. Minimap2: pairwise alignment for nucleotide sequences. *Bioinformatics* **34**, 3094-3100,

842   doi:10.1093/bioinformatics/bty191 (2018).

Figure 1. Cas9 HDR strand preference and gRNA selection. (A) Schematic representation of targeting (T) and non-targeting (NT) donor template designs. The targeting strand is complementary to the gRNA sequence, whereas the non-targeting strand contains the guide and PAM sequence (B) An EcoRI recognition site was inserted at a Cas9 cleavage site at 254 genomic loci in Jurkat and 239 genomic loci in HAP1 cells using either the T or NT strand as the donor template. RNP complexes (Alt-R S.p. Cas9 Nuclease complexed with Alt-R CRISPR-Cas9 crRNA and tracrRNA) were delivered at 4 µM along with 4 µM Alt-R Cas9 Electroporation Enhancer and 3 µM donor template by nucleofection. Total editing and perfect HDR was assessed via NGS. (C) Schematic of the gRNAs used to facilitate HDR insertion of an EcoRI site before the stop codon of GAPDH (TAA, red) in K562 cells using 13 guides around the desired HDR insertion location (blue, arrows indicate the 3' end). The cleavage sites and associated distance to the desired insertion location (green) for each gRNA are indicated above the sequence shown. Both the T and NT strand were tested. (D) RNP complexes (Alt-R S.p. Cas9 Nuclease, Alt-R CRISPR-Cas9 crRNA and tracrRNA) for the 13 guides targeting GAPDH were delivered at 2 µM along with 2 µM Alt-R Cas9 Electroporation Enhancer and 2 µM donor template designed to insert an EcoRI site before the stop codon by nucleofection to K562 cells. HDR and total editing were assessed via NGS. Data are represented as means ± S.E.M. of three biological replicates.
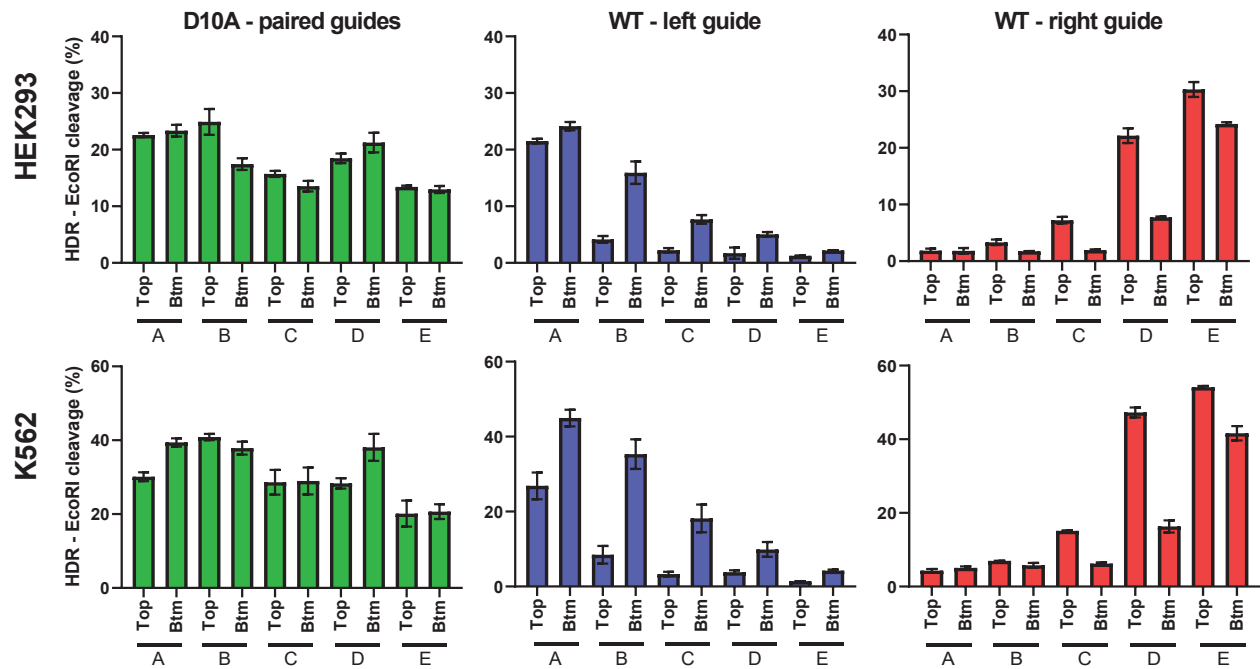
Figure 2. Cas9 D10A mediates efficient HDR distant from nick sites. (A) Ten HDR donor templates were designed with an EcoRI sequence positioned at varying distances (0-nt, 13-nt, 25-nt, 38-nt and 51-nt) from the left cleavage site of a paired-guide nickase design with a PAM-out orientation in HPRT1. ssODNs corresponding to the top and bottom (Btm) strand for each sequence were tested. Letters A-E indicate the position of the EcoRI insertion, the top strand ssODN is shown. (B) Cas9 D10A with gRNA pairs (left panel), or Cas9 WT with each of the individual gRNAs (middle and right panel) RNP complexes (Alt-R S.p. Cas9 D10A nickase or Alt-R S.p. Cas9 Nuclease complexed with Alt-R CRISPR-Cas9 crRNA and tracrRNA) were delivered at 4 µM (2 µM each RNP for nickase paired guides) along with 4 µM Alt-R Cas9 Electroporation Enhancer and 2 µM donor template by nucleofection to HEK293 cells (top) or K562 cells (bottom). HDR efficiency was evaluated by EcoRI cleavage of targeted amplicons. Data are represented as means ± S.E.M of three biological replicates for D10A and two biological replicates for WT.
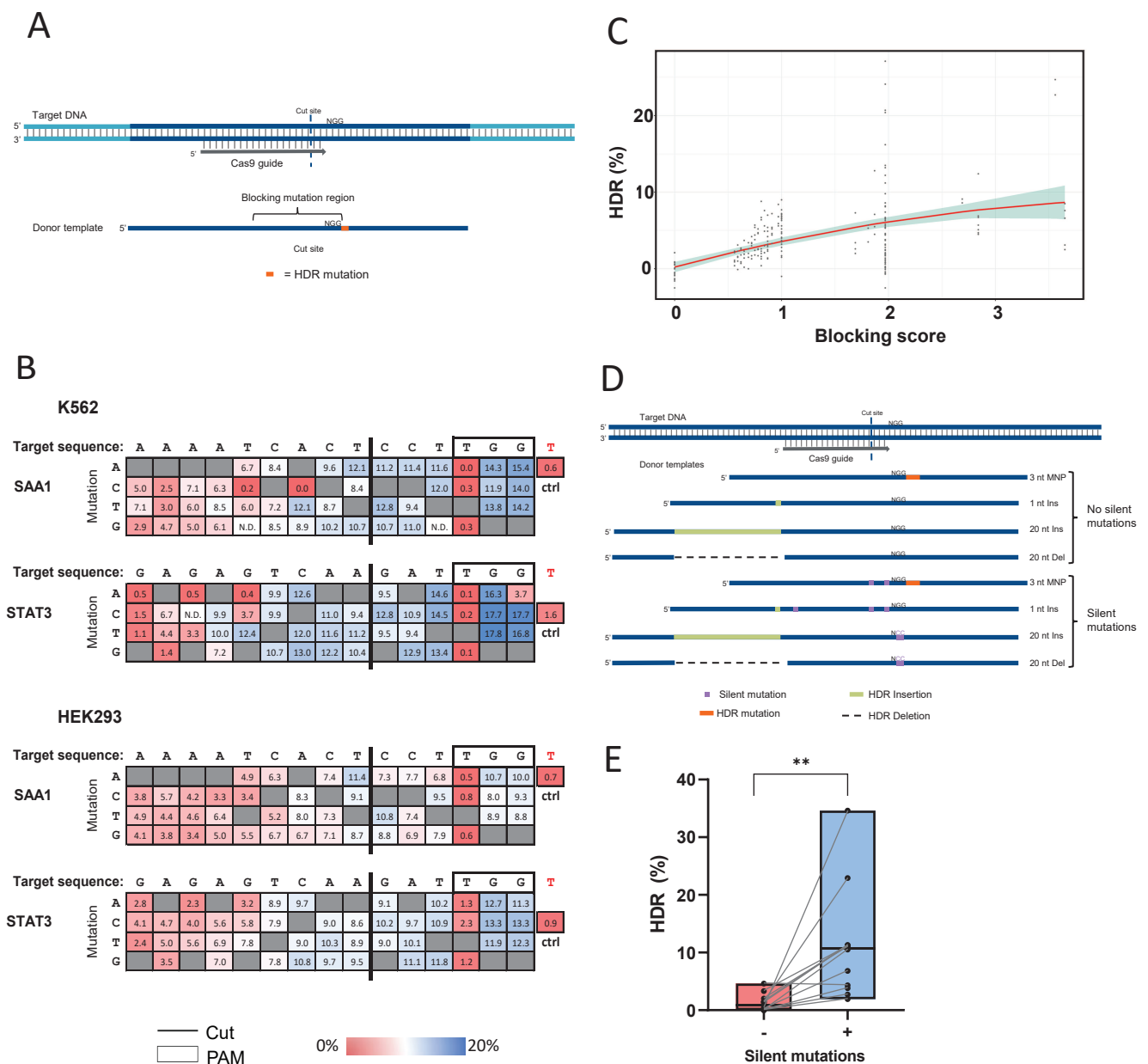
Figure 3. Optimizing placement and number of blocking mutations with Cas9. (A) Schematic representation of a desired HDR generated single base change (orange) 3' of the PAM. In addition to the desired HDR mutation, a single blocking mutation in the seed region of the guide or PAM to prevent Cas9 re-cleavage was included in donor templates. Each position in the region indicated was changed to every possible alternate base in a unique donor template that also contained the desired HDR mutation. (B) HDR donors for two genomic loci were tested in HEK293 and K562 cells. In each case the donor contained an HDR mutation 3' of the PAM, with or without a blocking mutation within the region indicated. HDR donors were delivered at 4 µM along with RNP complexes (Alt-R S.p. Cas9 Nuclease complexed with Alt-R CRISPR-Cas9 crRNA and tracrRNA) at 4 µM and with 4 µM Alt-R Cas9 Electroporation Enhancer by nucleofection. Each box represents the rate of perfect HDR including both the desired HDR mutation and blocking mutation (where applicable) as assessed by NGS. Blue indicates a higher HDR frequency, and red indicates a lower HDR frequency. (C) Blocking scores were calculated for 427 samples with known HDR frequencies and used to build a linear model (model = red line, standard error = blue highlight) to determine the optimum HDR efficiency. (D) Schematic representation of four unique HDR mutations that were designed using the Alt-R HDR Design tool either with or without the addition of silent mutations. (E) Four HDR mutations designed using the novel Alt-R HDR Design Tool with (+) or without (-) silent mutations were tested in HEK293, Hela, and Jurkat cells. RNP complexes (Alt-R S.p. Cas9 Nuclease, Alt-R CRISPR-Cas9 crRNA and tracrRNA) were delivered at 4 µM along with 4 µM Alt-R Electroporation Enhancer and 4 µM donor template in HEK293 and Jurkat cells by nucleofection. RNP complexes (Alt-R S.p. Cas9 Nuclease complexed with Alt-R CRISPR-Cas9 sgRNA) were delivered at 2 µM along with 2 µM Alt-R Cas9 Electroporation Enhancer and 2 µM donor template in Hela cells by nucleofection. Perfect HDR rates were determined by NGS.
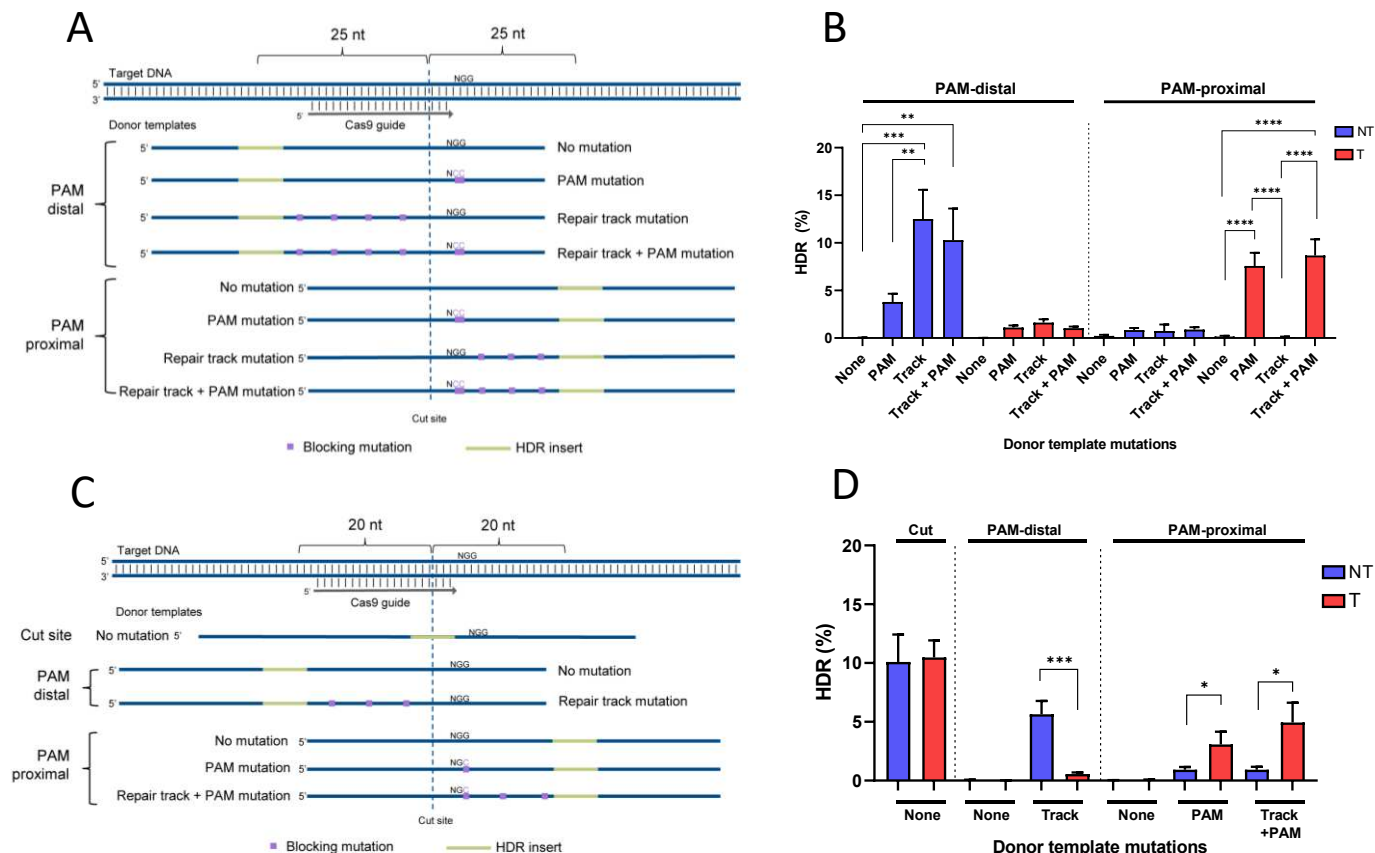
Figure 4. HDR mutation location determines donor strand preference. (A) Schematic representation of donor templates used to generate PAM-proximal and PAM-distal insertions 25 bases from a Cas9 cut site with no further mutations (None), PAM mutations (PAM), or mutations in the repair track with or without an additional PAM mutation. The NT strand ssODNs are shown. (B) Donor templates creating an EcoRI insertion 25 bases from the cut site at three genomic loci were delivered to Hela cells as the T or NT strand. Donor templates contained no further mutation (None), PAM mutation (PAM), or mutations in the repair track (Track). RNP complexes (Alt-R *S.p.* Cas9 Nuclease complexed with Alt-R CRISPR-Cas9 sgRNA) were delivered at 2 μM along with 2 μM Alt-R Cas9 Electroporation Enhancer and 0.5 μM donor template by nucleofection. Perfect HDR rates were determined by NGS. Data are represented as means $\pm$ S.E.M of the three sites tested. (C) Schematic representation of donor templates used to generate PAM-proximal and PAM-distal insertions 20 bases from a Cas9 cut site with no further mutations (None), PAM mutations (PAM), or mutations in the repair track with or without additional PAM mutation. The NT strand ssODNs are shown. (D) Donor templates creating an EcoRI insertion at the cut site or 20 bases PAM-proximal or PAM-distal to the Cas9 cut site for 12 genomic loci were tested in Jurkat cells as the T or NT strand. RNP complexes (Alt-R *S.p.* Cas9 Nuclease complexed with Alt-R CRISPR-Cas9 sgRNA) were delivered at 4 μM along with 4 μM Alt-R Cas9 Electroporation Enhancer and 3 μM donor template by nucleofection. Perfect HDR rates were determined by NGS. Data are represented as means $\pm$ S.E.M of the twelve sites tested.
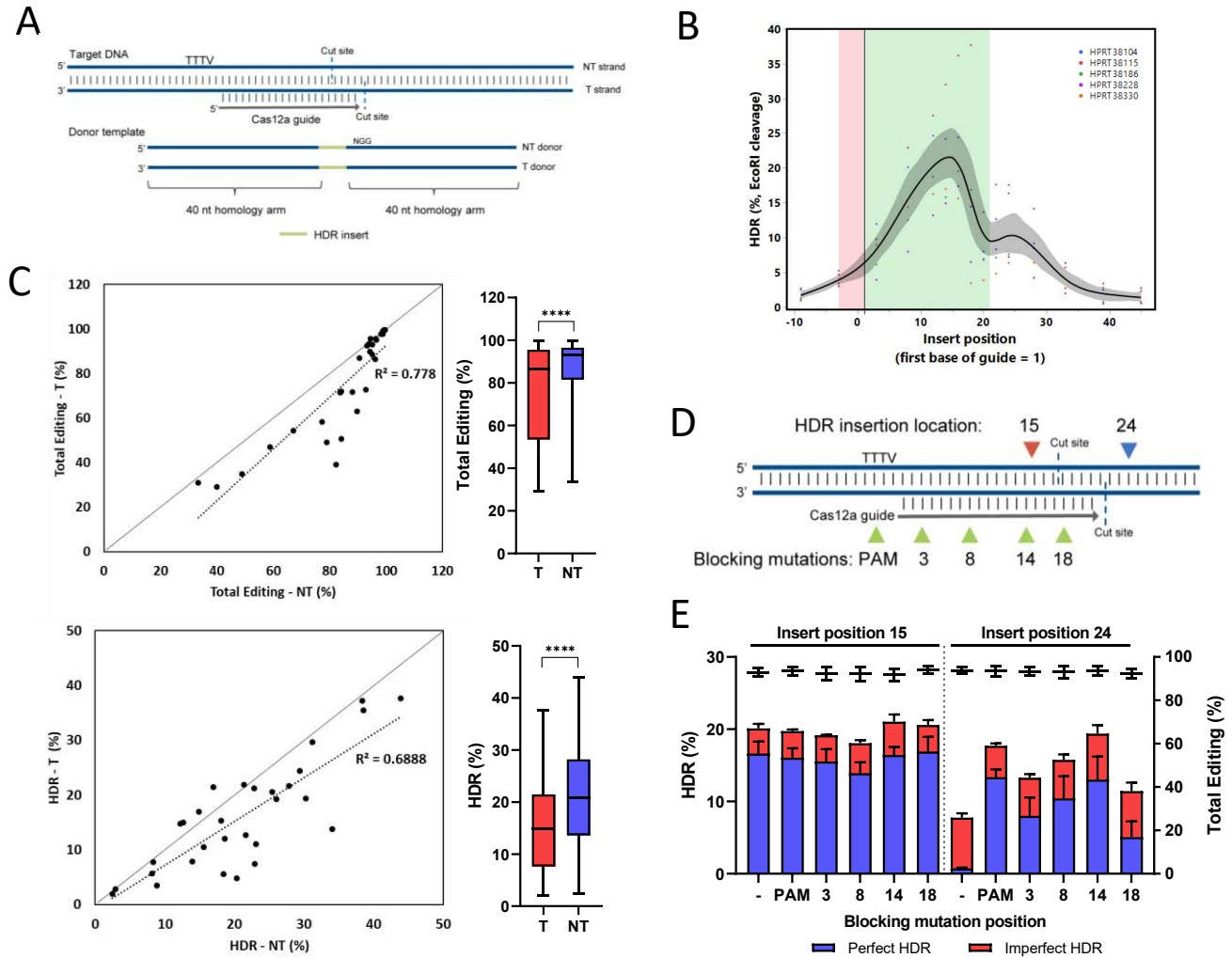
Figure 5. Cas12a HDR gRNA selection and strand preference. (A) Schematic representation of targeting (T) and non-targeting (NT) donor template designs. The T strand is complementary to the gRNA sequence, whereas the NT strand contains the guide and PAM sequence. (B) HDR donors were designed with an EcoRI insert sequence positioned at varying distances from the from the first base of the Cas12a guide RNA ranging from 10 bases in the 5' direction to 45 bases in the 3' direction for five genomic loci and delivered to HEK293 cells. RNP complexes (Alt-R *A.s.* Cas12a nuclease complexed with Alt-R CRISPR-Cas12a crRNA) were delivered at 5 μM along with 3 μM Alt-R Cpf1 Electroporation Enhancer and 3 μM donor template by nucleofection. HDR rates were assessed via EcoRI cleavage of targeted amplicons. The 21-bases where the gRNA targets is highlighted in green. The 4 base 'TTTV' PAM is highlighted in red. The gray shading indicates the confidence of fit. (C) An EcoRI restriction digest recognition site was inserted at position 16 of the gRNA sequence in 15 genomic loci in Jurkat and HAP1 cells using either the T or NT strand as the donor template and the combined results graphed together. RNP complexes (Alt-R *A.s.* Cas12a *Ultra* nuclease complexed with Alt-R CRISPR-Cas12a crRNA) were delivered at 1 μM along with 3 μM Alt-R Cpf1 Electroporation Enhancer and 3 μM donor template by nucleofection. Total editing and perfect HDR was assessed via NGS. (D) Donors for two genomic loci were designed to insert an EcoRI site within the Cas12a guide sequence (position 15 of the guide) or outside of the guide sequence (24 bases from the start of the guide). ssODNs for these two insert locations were designed with blocking mutations in the PAM or guide sequence. The positions where blocking mutations were incorporated are indicated. (E) Donor templates for two genomic loci in *HPRT1* were tested in Jurkat and Hela cells. RNP complexes (Alt-R *A.s.* Cas12a *Ultra* complexed with Alt-R CRISPR-Cas12a crRNA) were delivered at 2 μM along with 2 μM Alt-R Cpf1 Electroporation Enhancer and 3 μM donor template by nucleofection. HDR rates were assessed via NGS. Perfect HDR (blue), imperfect HDR (red) and total editing, which includes NHEJ events (black) are shown. Data are represented as means ± S.E.M.
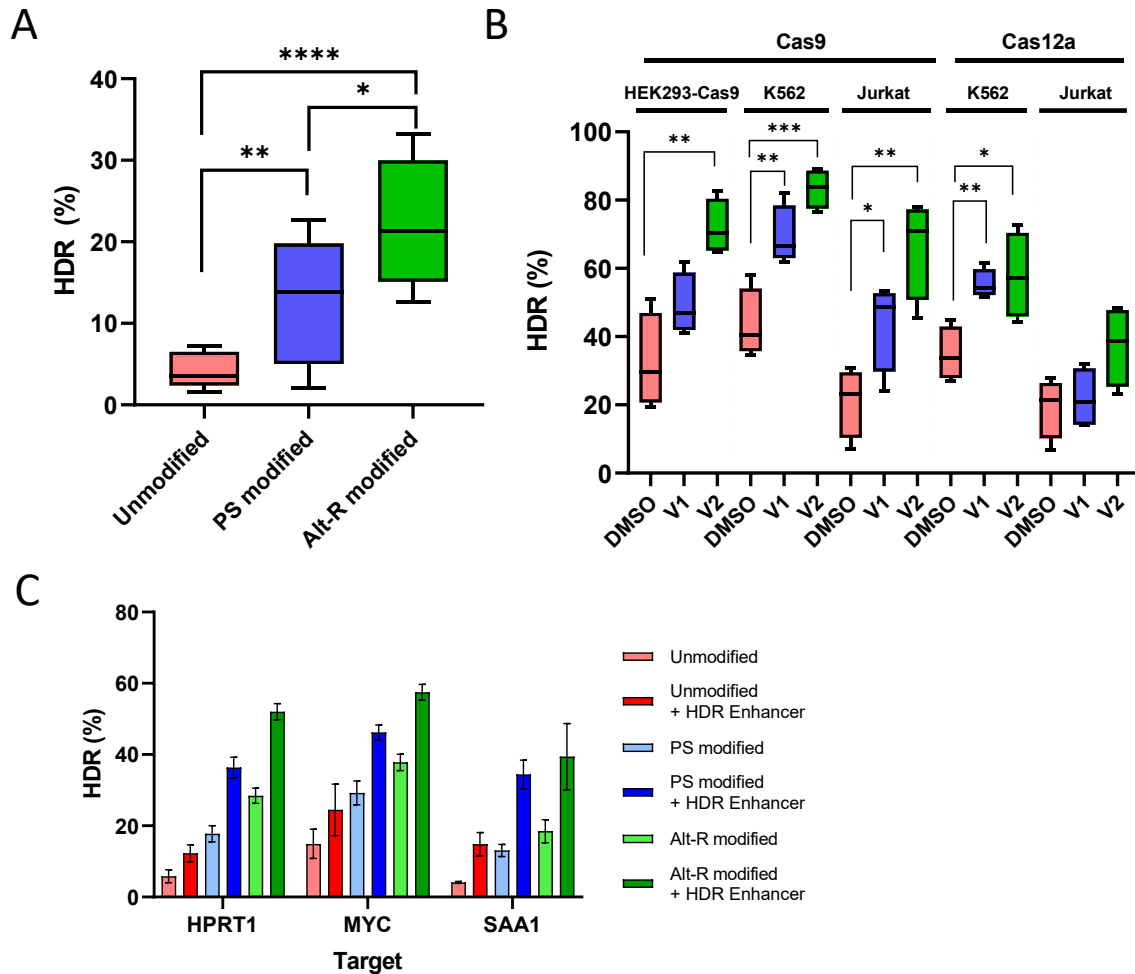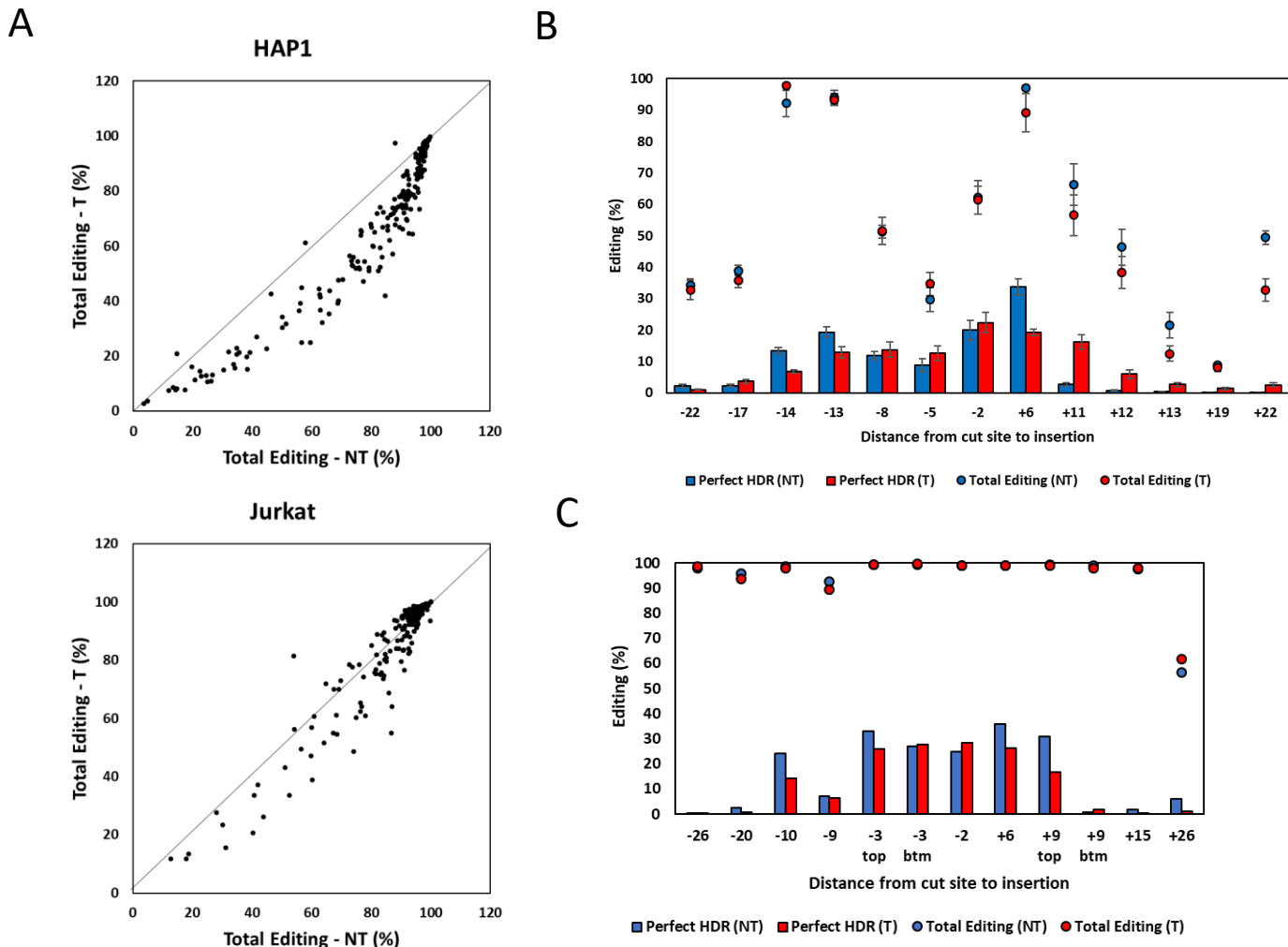
Figure 6. Alt-R modified HDR Donor oligos and Alt-R HDR Enhancer reagents further improve HDR. (A) Hela cells were transfected with 2 µM Cas9 RNP complexes (Alt-R *S.p.* HiFi Cas9 Nuclease complexed with Alt-R CRISPR-Cas9 sgRNA) targeting 8 genomic loci along with 0.5 µM HDR donor template and 2 µM Alt-R Cas9 Electroporation Enhancer by nucleofection. Donor templates contained no modifications (Unmodified), 2 phosphorothioate linkages between the first and last three bases of the template (PS modified), or the Alt-R HDR modification (Alt-R modified). HDR efficiency was measured by NGS. (B) HDR donor templates for four genomic loci for Cas9 and four genomic loci for Cas12a were designed to insert an EcoRI site at the cut site (Cas9) or at the 16th base of the guide (Cas12a). To test lipofection delivery, gRNA complexes were delivered at 10 nM gRNA (Alt-R Cas9 crRNA and tracrRNA) with 3 nM donor template into HEK293-Cas9 cells. For Cas9 sites, K562 and Jurkat cells were transfected with 2 µM RNP (Alt-R *S.p.* Cas9 Nuclease complexed with Alt-R CRISPR-Cas9 crRNA and tracrRNA), 3 µM Alt-R Cas9 Electroporation Enhancer, and 3 µM donor template. For Cas12a sites, K562 and Jurkat cells were transfected with 2 µM RNP (Alt-R *A.s.* Cas12a *Ultra* complexed with Alt-R CRISPR-Cas12a crRNA), 3 µM Alt-R Cpf1 Electroporation Enhancer, and 3 µM donor template. Immediately after transfection, cells were plated in media containing a DMSO control, 30 µM Alt-R HDR Enhancer V1, or 1 µM Alt-R HDR Enhancer V2 and media was changed after 24 hours. HDR efficiency was measured by NGS. (C) Hela cells were transfected with 2 µM Cas9 RNP complexes (Alt-R *S.p.* HiFi Cas9 Nuclease complexed with Alt-R CRISPR-Cas9 crRNA and tracrRNA) targeting 3 genomic loci along with 0.5 µM HDR donor template and 2 µM Alt-R Cas9 Electroporation Enhancer by nucleofection. Donor templates were unmodified, PS modified, or Alt-R modified. Immediately after electroporation, cells were plated in media with or without 30 µM Alt-R HDR Enhancer (V1) and media was changed after 24 hours. HDR efficiency was measured by NGS. Data are represented as means $\pm$ S.E.M of three biological replicates.
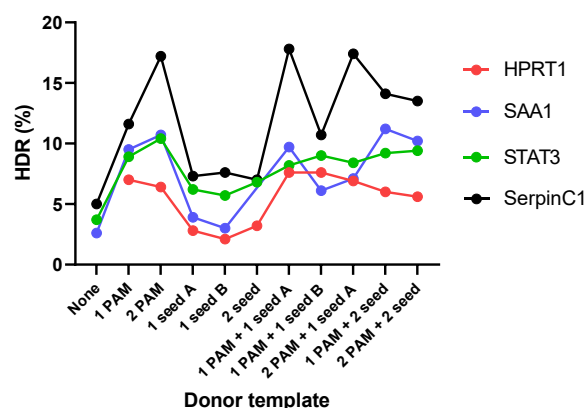
Supplemental Figure 1 (A) EcoRI restriction digest recognition site (GAATTC) was inserted at the Cas9 cleavage site of 254 genomic loci in Jurkat and 239 genomic loci in HAP1 cells using either the targeting (T) or non-targeting (NT) strand as the donor template. RNP complexes (Alt-R *S.p.* Cas9 Nuclease complexed with Alt-R CRISPR-Cas9 crRNA and tracrRNA) were delivered at 4 µM along with 4 µM Alt-R Cas9 Electroporation Enhancer and 3 µM donor template by nucleofection. Total editing was assessed via NGS. (B) Insertion of an EcoRI site before the stop codon of GAPDH in HEK293 cells using guides around the desired HDR insertion location. The cleavage sites and associated distance to the desired insertion location for each guide are indicated above the sequence shown. Both the T and NT strand were tested. RNP complexes (Alt-R *S.p.* Cas9 Nuclease complexed with Alt-R CRISPR-Cas9 crRNA and tracrRNA) were delivered at 2 µM along with 2 µM Alt-R Cas9 Electroporation Enhancer and 2 µM donor template by nucleofection. HDR and total editing were assessed via NGS. Data are represented as means ± S.E.M. of three technical replicates. (C) Insertion of an EcoRI site at the TNPO3 locus in HEK293 cells using guides around the desired HDR insertion location. The distance from each cleavage site to the desired insertion location for each guide are indicated on the x-axis. Two pairs of guides cut at the same location, but on opposite strands. The strand containing the guide is indicated as top or bottom (btm). Both the T and NT strand were tested. RNP complexes (Alt-R *S.p.* Cas9 Nuclease complexed with Alt-R CRISPR-Cas9 crRNA and tracrRNA) were delivered at 2 µM along with 2 µM Alt-R Cas9 Electroporation Enhancer and 2 µM donor template by nucleofection. HDR and total editing were assessed via NGS.
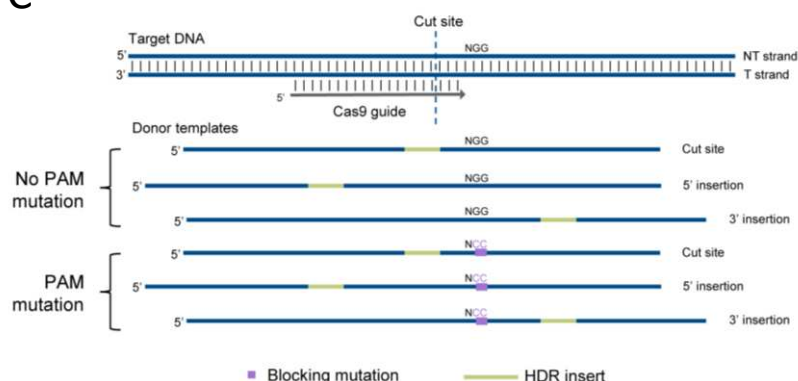
Supplemental Figure 2 HDR using Cas9 D10A nickase compared to WT Cas9 and Cas9 H840A nickase (A) Schematics showing gRNA pairs in PAM-out orientation (top panel) or PAM-in orientation (bottom panel). NGG PAMs are red, protospacers are underlined. Spacing between paired gRNAs is defined by the distance between targeted nick sites as indicated in the diagram. (B) RNP complexes consisting of gRNA pairs in different orientation and spacing targeting the *HPRT1* locus were delivered into HEK293 cells with Cas9 D10A or H840A proteins via lipofection and total editing was measured by T7EI cleavage. (C) HDR mediated by Cas9 WT (left panel) or Cas9 H840A (right panel) with paired gRNAs. Cas9 WT and Cas9 H840A were used in combination with gRNA pairs targeting *HPRT1* 51-nt PAM-out site. RNP complexes (Alt-R *S.p.* Cas9 Nuclease or Alt-R *S.p.* Cas9 H840A nickase complexed with Alt-R CRISPR-Cas9 crRNA and tracrRNA) were delivered at 4 µM (2 µM each RNP for nickase paired guides) along with 4 µM Alt-R Cas9 Electroporation Enhancer and 2 µM donor template by nucleofection. The same set of ssODNs homologous to either the top or bottom (Btm) strand as shown in Figure 2 were used to insert an EcoRI site along the target region. HDR was assessed via EcoRI cleavage. (D) Schematics of HDR donor oligos. HDR donor sequences were designed to insert an EcoRI site at 7 positions along the AAVS1 46-nt PAM-out target region. (E) HDR performance of donor oligos in HEK293 cells. Cas9 D10A with two guides, or Cas9 WT with each of the individual guides were used to induce double strand breaks. Bar charts are showing the HDR rate using indicated oligos homologous to either the top or bottom strand. Data are represented as means ± S.E.M of technical triplicates.

A

Donor ID	Guide	ACCTCTGGAAAAAGGTAAGA
None		GAACTGTAACCTCTGGAAAAAGGTAAGA**GGGA**TGAGCTTTCCCCTTGCCT
1 PAM		GAACTGTAACCTCTGGAAAAAGGTAAGAG**GC**ATGAGCTTTCCCCTTGCCT
2 PAM		GAACTGTAACCTCTGGAAAAAGGTAAGAG**CC**ATGAGCTTTCCCCTTGCCT
1 seed A		GAACTGTAACCTCTGGAAAAAGGTAA**T**AGGGATGAGCTTTCCCCTTGCCT
1 seed B		GAACTGTAACCTCTGGAAAAAGGT**C**AGAGGGATGAGCTTTCCCCTTGCCT
2 seed		GAACTGTAACCTCTGGAAAAAGGT**CA**TAGGGATGAGCTTTCCCCTTGCCT
1 PAM + 1 seed A		GAACTGTAACCTCTGGAAAAAGGTAA**T**AGG**C**ATGAGCTTTCCCCTTGCCT
1 PAM + 1 seed B		GAACTGTAACCTCTGGAAAAAGGT**C**AGAGG**C**ATGAGCTTTCCCCTTGCCT
2 PAM + 1 seed A		GAACTGTAACCTCTGGAAAAAGGTAA**T**AG**CC**ATGAGCTTTCCCCTTGCCT
1 PAM + 2 seed		GAACTGTAACCTCTGGAAAAAGGT**CA**TAGG**C**ATGAGCTTTCCCCTTGCCT
2 PAM + 2 seed		GAACTGTAACCTCTGGAAAAAGGT**CA**TAG**CC**ATGAGCTTTCCCCTTGCCT

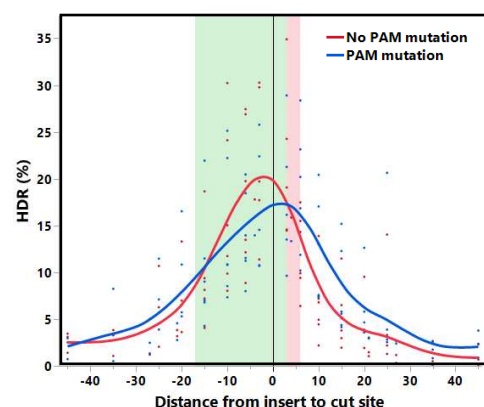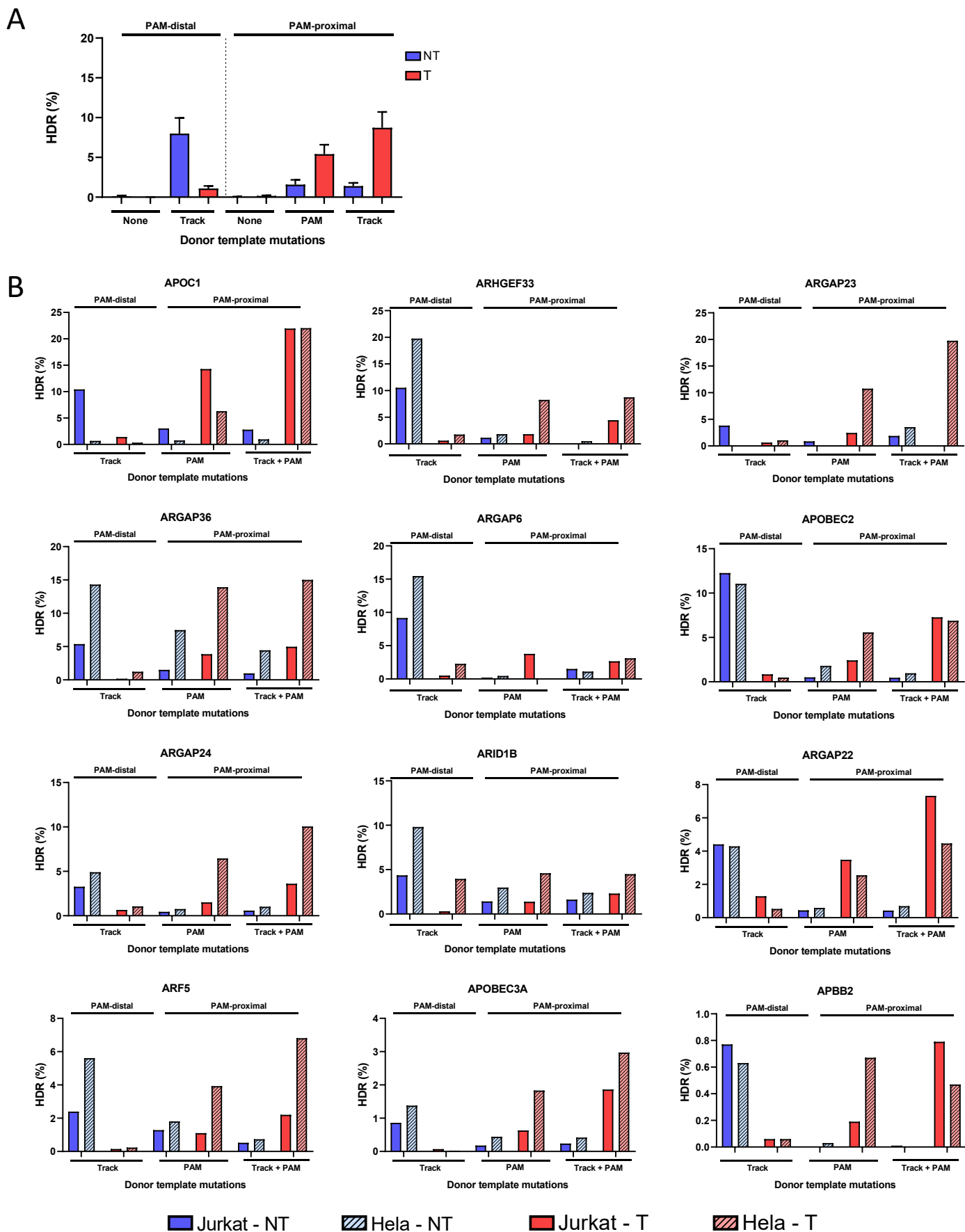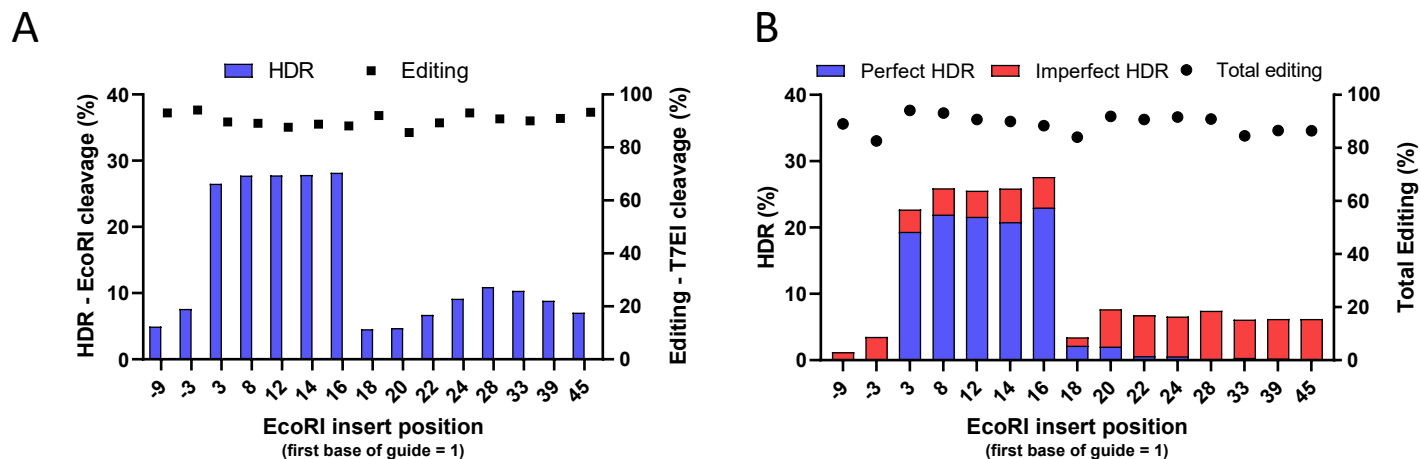**blocking mutation**; **desired HDR SNP**; **PAM**

B

C

D

Supplemental Figure 3 (A) Example sequence of site SERPINC1 showing the various blocking mutation(s) tested. The Cas9 guide is shown above the sequence, and the PAM is bolded. The intended HDR mutation is in red and blocking mutations are shown in blue. (B) Donor templates for four target loci following the design strategy shown in panel A were delivered to Jurkat cells at 4 µM along with RNP complexes (Alt-R *S.p.* Cas9 Nuclease complexed with Alt-R CRISPR-Cas9 crRNA and tracrRNA) at 4 µM and with 4 µM Alt-R Cas9 Electroporation Enhancer by nucleofection. SNP conversion of the desired HDR mutation 3' of the PAM was determined by NGS. (C) Schematic representation of donor templates used to an EcoRI insert sequence positioned at varying distances from the Cas9 cleavage site, ranging up to 45 bases in either the 5' or 3' direction. Donor templates were designed with and without a mutation in the PAM ('NGG' to 'NCC') to prevent Cas9 re-cleavage. (D) HDR performance of donor templates for four genomic loci in Jurkat cells and two genomic loci in HEK293 cells. Negative values indicate the insertion was 5' (PAM-distal) of the cut site, whereas positive values indicate the insertion was 3' (PAM-proximal) of the cut site. RNP complexes (Alt-R *S.p.* Cas9 Nuclease complexed with Alt-R CRISPR-Cas9 crRNA and tracrRNA) were delivered at 4 µM along with 4 µM Alt-R Cas9 Electroporation Enhancer and 4 µM donor template by nucleofection. HDR rates were assessed via EcoRI cleavage of targeted amplicons.

Supplemental Figure 4 (A) Donor templates creating an EcoRI insertion at the cut site or 20 bases PAM-proximal or PAM-distal to the Cas9 cut site for 12 genomic loci were tested in Hela cells as the targeting (T) or non-targeting (NT) strand. Donor templates for the PAM-distal insert contained repair track mutations. Donor templates for the PAM-proximal insert contained either PAM mutation or repair track plus PAM mutations. RNP complexes (Alt-R *S.p.* Cas9 Nuclease complexed with Alt-R CRISPR-Cas9 sgRNA) were delivered at 4 µM along with 4 µM Alt-R Cas9 Electroporation Enhancer and 3 µM donor template by nucleofection. Perfect HDR rates were determined by NGS. Data are represented as means ± S.E.M. (B) Individual plots of the 12 sites tested in HeLa and Jurkat cells.

Supplemental Figure 5 Site HPRT 38330 from Figure 5B was delivered as an RNP complex (Alt-R *A.s.* Cas12a *Ultra* nuclease complexed with Alt-R CRISPR-Cas12a crRNA) at 2 µM along with 3 µM Alt-R Cpf1 Electroporation Enhancer and 3 µM Alt-R modified donor templates by nucleofection to Jurkat cells. HDR was measured by EcoRI cleavage (A) and NGS analysis (B) to determine the frequency of perfect HDR (blue) relative to imperfect HDR (red) and total editing (black dots).